Realization of the Frolov cubature formula via orthogonal Chebyshev-Frolov lattices

Christopher Kacwin

Born 31st of May 1992 in Hamburg, Germany

23rd August 2016

Master's Thesis Mathematics

Advisor: Prof. Dr. Michael Griebel

Second Advisor: Dr. Tino Ullrich

Institut für Numerische Simulation Bonn

Mathematisch-Naturwissenschaftliche Fakultät der

Rheinischen Friedrich-Wilhelms-Universität Bonn

Contents

1 Introduction

Numerical integration is a branch of numerical analysis which is concerned with the calculation of the numerical value of a definite integral. Often, this cannot be done analytically since the anti-derivative is either not known or simply no closed form exists. It may also be the case that only specific function values of the integrand are accessible, obtained e.g. by a sampling method. For this reason, cubature formulas are popular numerical integration schemes, because they only use function values to approximate an integral. For a given integration domain $\Omega \subset \mathbb{R}^d$ a cubature formula has the form

$$A_N(f) = \sum_{i=1}^{N} \lambda_i f(x_i) \approx \int_\Omega f(x) \mathrm{d}x \, , \tag{1.1}$$

where $\lambda_1, \ldots, \lambda_N \in \mathbb{R}$ are called weights and $x_1, \ldots, x_N \in \Omega$ are called integration points or nodes. The integration error for a specific function f is then given by

$$e(A_N; f) = \left| A_N(f) - \int_\Omega f(x) \mathrm{d}x \right| \tag{1.2}$$

and one is usually interested in quantifying the decay for increasing N. More precisely, for a given function class $\mathbf{F}$, one tries to describe the *worst case error*

$$E(A_N; \mathbf{F}) = \sup_{f \in \mathbf{F}} e(A_N; f) \tag{1.3}$$

of a given cubature formula A_N and, ideally, determine the convergence rate with respect to N. A cubature formula A_N is called optimal with respect to $\mathbf{F}$ if it has the same asymptotic behavior as the optimal error bound given by

$$E_N(\mathbf{F}) = \inf_{A_N} E(A_N; \mathbf{F}) \tag{1.4}$$

which describes the inherent difficulty of estimating an integral in F with cubature formulas using N integration points and weights. The optimal error bound is usually obtained by first finding a lower bound on $E_N(\mathbf{F})$ using "fooling functions", i.e. functions which belong to $\mathbf{F}$ but have small values near integration points (see for instance [5, Section 8]). Then, a cubature formula is constructed which has the same convergence rate as this lower bound. This cubature formula is then of course optimal with respect to $\mathbf{F}$. While the univariate case is understood really well, finding optimal cubature formulas for high dimensions is an ongoing research topic to this day.

Of particular interest in this thesis are function spaces of dominating mixed smoothness such as the Sobolev spaces of dominating mixed smoothness H^r_{mix}, or the more general Besov spaces of dominating mixed smoothness $S^r_{p,\theta}B$ (the definitions can be found in Section 6).

Lower bounds for these classes are known for $1 \le p, \theta \le \infty$, $r > 1/p$ ($r > 1/2$ in the H_{mix}^r case) and given by

$$E_N(H_{\mathrm{mix}}^r) \gtrsim N^{-r} \log^{\frac{d-1}{2}}(N) \tag{1.5}$$

$$E_N(S_{p,\theta}^r B) \gtrsim N^{-r} \log^{(d-1)(1-1/\theta)}(N) \tag{1.6}$$

and can be found e.g in [5, Theorem 8.3].

Popular methods for numerical integration are digital nets [2, 8] and Smolyak's algorithm, also known as the sparse grids method [19, 1]. Digital nets belong to the quasi-Monte Carlo methods, which means that they have equal weights $\lambda_i = 1/N$. While it is known that the sparse grids method SG_N has convergence rates [6]

$$E(SG_N; H_{\mathrm{mix}}^r) \asymp N^{-r} \log^{(d-1)(r+1/2)}(N) \tag{1.7}$$

$$E(SG_N; S_{p,\theta}^r B) \asymp N^{-r} \log^{(d-1)(r+1-1/\theta)}(N) \tag{1.8}$$

which is worse than the lower bounds (1.5) and (1.6), it is still being used frequently, because the difference is slim for low dimensions and an explicit construction of the integration points and weights is possible. Digital nets achieve the optimal convergence rates (1.5) and (1.6) for the range $1/p < r < 2$, which was recently shown in [10]. However, the construction is more involved and connected to number theory.

We will focus on the Frolov cubature formula introduced by K. K. Frolov in [7], which dates back to 1976 and recently returned to academic focus due to its optimal convergence rate for various function classes including (1.5) for H_{mix}^r and (1.6) for $S_{p,\theta}^r B$ for the whole range $1/p < r < \infty$. For a given lattice $\Gamma \subset \mathbb{R}^d$, it is defined as

$$\Phi_\Gamma(f) = \det(\Gamma) \sum_{x \in \Gamma \cap \Omega} f(x). \tag{1.9}$$

This cubature formula has integration points $\{x_i\}_{i=1}^N$ which are an arbitrary enumeration of $\Gamma \cap \Omega$, and uniform weights $\lambda_i = \det(\Gamma)$, where $\det(\Gamma)$ is the determinant of the lattice Γ and describes the density of its lattice points. However, it is not a quasi-Monte Carlo method because the weights do not sum up to one in general, i.e. $\det(\Gamma) \ne 1/N$. The theory behind this formula recently has been further developed in [23, 4, 3], but numerical simulations are still rare, because there are two major obstacles to overcome if one wants to put this method into practice. First, the lattice Γ used in the Frolov cubature formula needs to have the admissibility property [18]

$$\inf_{\gamma \in \Gamma \backslash \{0\}} \left| \prod_{i=1}^d \gamma_i \right| > 0 \tag{1.10}$$

to guarantee optimal convergence behavior. Finding proper admissible lattices is a problem on its own and requires deep considerations in number theory. Second, this formula is not

explicit, in the sense that there is no general procedure available to enumerate the set of nodes $\Gamma \cap \Omega$. Additionally, the difficulty of these problems rises with increasing dimension d.

The main effort of this master's thesis was to implement the Frolov cubature formula and discuss its numerical performance as well as its practicability. In order to do this, we will begin with the construction of the Frolov cubature formula, and therefore the next three sections are dedicated to the study of lattices. Starting with general facts about lattices in Section 2, we gradually get more specific, introducing Vandermonde-type lattices in Section 3. This will be done using basic algebra and number theory. Section 4 is about Chebyshev lattices. My search for a decent lattice representation of these lattices led me a new result which is also a main result of this thesis, namely that Chebyshev lattices are orthogonal. This result was already published as a preprint on the arxiv [11] as a joint work with Dipl.-Mat. Jens Oettershagen (Bonn) and Dr. Tino Ullrich (Bonn). Chebyshev lattices are admissible if the dimension d is a power of 2, i.e. $d = 2^m, m \in \mathbb{N}$, and we will also call these lattices *Chebyshev-Frolov lattices*. The Frolov cubature formula based on these admissible lattices achieves optimal convergence rates for Besov spaces of dominating mixed smoothness. In Section 5 we discuss an efficient enumeration algorithm which assembles the integration points needed for the Frolov cubature formula. The orthogonality property of the Chebyshev lattices can be used to significantly reduce the complexity of this algorithm, which in turn lets us put the Frolov cubature formula to practice for the dimensions $d \in \{2, 4, 8, 16\}$. To our knowledge, this has not been done prior to this work. In Section 6 we recall the definition of Sobolev and Besov spaces of dominating mixed smoothness, state convergence results of the Frolov cubature formula on these function classes, and give a heuristic regarding the effect of the chosen lattice in question on the convergence rate. It turns out that the Chebyshev-Frolov lattices behave well in this context. Section 7 contains numerical experiments done with the Frolov cubature formula, based on Chebyshev-Frolov lattices in dimensions $d \in \{2, 4, 8, 16\}$. Various test functions with different regularities are used to verify the theoretical results concerning the Frolov cubature formula, as well as compare it with the sparse grids method. In the end, we give a short outlook on open questions and future goals.

Notation. We denote by $\mathbb{N}$ the natural numbers and $\mathbb{N}_0 = \mathbb{N} \cup \{0\}$, $\mathbb{Z}$ denotes the integers, $\mathbb{R}$ the real numbers, and $\mathbb{C}$ the complex numbers. For a real positive number b, we denote by $\lfloor b \rceil$ the largest integer less or equal to b. The letter d is always reserved for the underlying dimension in $\mathbb{R}, \mathbb{Z}$ etc. We denote with (x, y) the usual Euclidean inner product in $\mathbb{R}^d$. With $|\cdot|_p$ and $\|\cdot\|_p$ we denote the (d-dimensional) discrete ℓ_p-norm of an element of $\mathbb{R}^d$ and the continuous L_p-norm of a real-valued function on $\mathbb{R}^d$ respectively. With $\mathcal{F}$ we denote the Fourier transform given by $\mathcal{F}f(\xi) := (2\pi)^{-d/2} \int_{\mathbb{R}^d} f(x) \exp(-i(x, \xi)) \, dx$ for a function $f \in L_1(\mathbb{R}^d)$ and $\xi \in \mathbb{R}^d$. For two functions f and g which may both be univariate or multivariate, we denote by $f * g(\cdot)$ the convolution of f and g. For two sequences of real numbers a_n and b_n we will write $a_n \lesssim b_n$ if there exists a constant $c > 0$ such that $a_n \leq c \, b_n$ for all n. We will write $a_n \asymp b_n$ if $a_n \lesssim b_n$ and $b_n \lesssim a_n$. With $\mathrm{GL}_d(\mathbb{R})$ we denote the group of invertible $d \times d$ matrices over $\mathbb{R}$, and with $\mathrm{SL}_d(\mathbb{Z})$ we denote the group of invertible $d \times d$

matrices over $\mathbb{Z}$ with unit determinant. The notation $A = (a_1 | \cdots | a_d)$, where $a_1, \ldots, a_d \in \mathbb{R}^d$, stands for the $d \times d$ matrix which has a_i as its i-th column. The notation $D := \mathrm{diag}(x_1, ..., x_d)$ with $x = (x_1, ..., x_d) \in \mathbb{R}^d$ refers to the diagonal matrix $D \in \mathbb{R}^{d \times d}$ with x on the diagonal. For a matrix $A \in \mathbb{R}^{d \times d}$ and a set $X \subset \mathbb{R}^d$ we denote by AX or $A(X)$ the set $\{Ax : x \in X\}$. The matrix $A^\top$ is the transpose of A, A^{-1} is the inverse of A, and $A^{-\top}$ denotes the inverse transpose of A. By $\mathbb{Z}[x]$ and $\mathbb{Q}[x]$ we denote the ring of polynomials with integer coefficients and with rational coefficients respectively, and with $\mathbb{Z}_b[x]$ for $b \in \mathbb{N}$ we refer to the ring of polynomials over the cyclic group $\mathbb{Z}_b = \{0, \ldots, b-1\}$. For an algebraic number $\alpha \in \mathbb{C}$ and a subring R of $\mathbb{C}$, we denote by $R[\alpha]$ the corresponding ring extension. If K is a subfield of $\mathbb{C}$ we denote by $K(\alpha)$ the corresponding field extension, and for two fields $K \subset L$ we also use the notation L/K.

2 General facts about lattices

In this section we will briefly recall the precise notions of a lattice, its dual lattice, orthogonal and admissible lattices.

Definition 2.1 (Lattice). *A (full-rank) lattice $\Gamma \subset \mathbb{R}^d$ is a subgroup of $\mathbb{R}^d$ which is isomorphic to $\mathbb{Z}^d$ and spans the real vector space $\mathbb{R}^d$. A set $\{a_1, ..., a_d\} \subset \Gamma$ such that $\mathrm{span}_{\mathbb{Z}}\{a_1, ..., a_d\} = \{\sum_{i=1}^d k_i a_i : k \in \mathbb{Z}^d\} = \Gamma$ is called a generating set of Γ. The matrix $A = (a_1|\cdots|a_d) \in GL_d(\mathbb{R})$ is called a lattice representation for Γ, i.e. we can write*

$$\Gamma := \{Ak : k \in \mathbb{Z}^d\} = A(\mathbb{Z}^d). \tag{2.1}$$

A lattice has many different representations, as shown in the next theorem.

Theorem 2.2. *Let $A, B \in GL_d(\mathbb{R})$ and $\Gamma_A = A(\mathbb{Z}^d), \Gamma_B = B(\mathbb{Z}^d)$ be the corresponding lattices. We have $\Gamma_A = \Gamma_B$ if and only if there exists a matrix U with integer entries that satisfies*

$$\det U = \pm 1, \quad A = BU. \tag{2.2}$$

Proof. Assume that $\Gamma_A = \Gamma_B$. Since $A(\mathbb{Z}^d) = B(\mathbb{Z}^d)$ we also have $\mathbb{Z}^d = B^{-1}A(\mathbb{Z}^d) = A^{-1}B(\mathbb{Z}^d)$, and this implies that $U = B^{-1}A$ and U^{-1} have integer entries. Then, necessarily, $\det U = \pm 1$. Now assume that $U = B^{-1}A$ has integer entries and $\det U = \pm 1$. It is clear that we have $U(\mathbb{Z}^d) = \mathbb{Z}^d$ and subsequently

$$\Gamma_A = A(\mathbb{Z}^d) = BU(\mathbb{Z}^d) = B(\mathbb{Z}^d) = \Gamma_B. \quad \square$$

This means that two lattice representation matrices of a lattice Γ differ only by a unimodular matrix U, giving rise to the question which lattice representation is favorable from the numerical point of view, cf. Figure 1. In the special case of orthogonal lattices, an orthogonal representation stands out obviously.

Definition 2.3 (Orthogonal lattice). *A lattice Γ is called orthogonal if there exists a generating matrix $A \in GL_d(\mathbb{R})$ which has orthogonal column vectors.*

In general, the computation of an orthogonal representation for an orthogonal lattice is performed by a discrete variant of the Gram-Schmidt method, e.g. the Lenstra-Lenstra-Lovász–lattice basis reduction algorithm (LLL) [13] or its modifications. However, in the case of Chebyshev-lattices an orthogonal basis can be determined a priori without any additional computational effort, as we will show in Section 4.

A direct consequence of Theorem 2.2 is the invariance of $|\det A|$ for any lattice representation A corresponding to Γ. This leads us to the following definition.
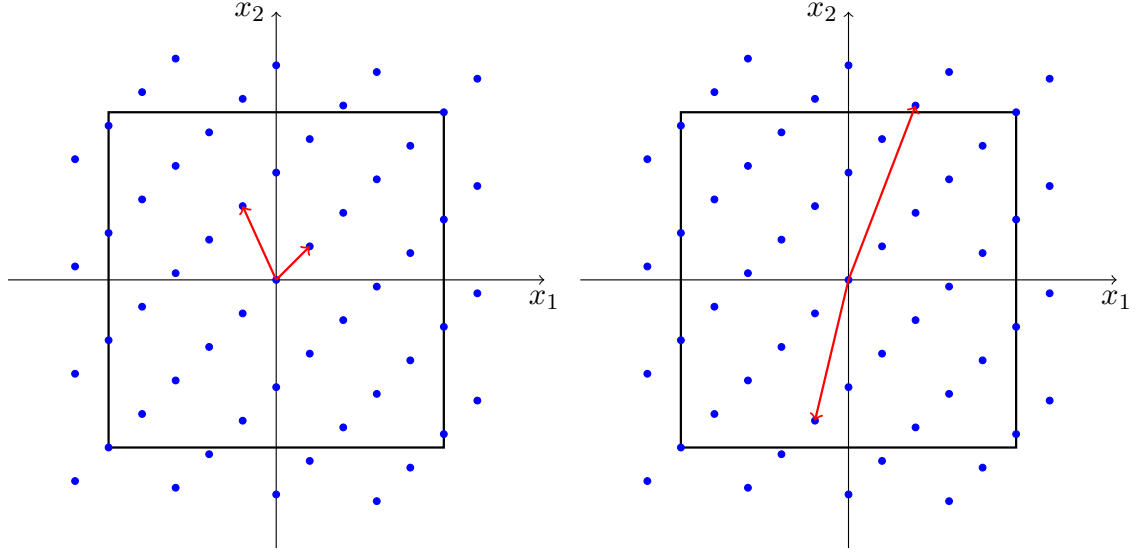
Figure 1: Equivalent lattice representations within the unit cube $\Omega = [-1/2, 1/2]^2$. The highlighted lattice elements are the columns of the corresponding lattice representation.

Definition 2.4 (Determinant). *For a lattice Γ and a corresponding lattice representation A, the determinant of Γ is defined as*

$$\det(\Gamma) = |\det A|. \tag{2.3}$$

Let us further introduce the dual lattice.

Definition 2.5 (Dual lattice). *Given the lattice Γ we define the dual lattice $\Gamma^\perp$ as*

$$\Gamma^\perp = \{x \in \mathbb{R}^d : (x, y) \in \mathbb{Z} \text{ for all } y \in \Gamma\}. \tag{2.4}$$

The following lemma states properties of the dual lattice which immediately follow from the definition.

Lemma 2.6. *We consider a lattice Γ and its dual lattice $\Gamma^\perp$. Then we have*

- $\Gamma^\perp$ *is a lattice,*

- $(\Gamma^\perp)^\perp = \Gamma$,

- $\det(\Gamma^\perp) = \det(\Gamma)^{-1}$,

- *If A is a lattice representation for Γ then $A^{-\top}$ is a lattice representation for $\Gamma^\perp$.*
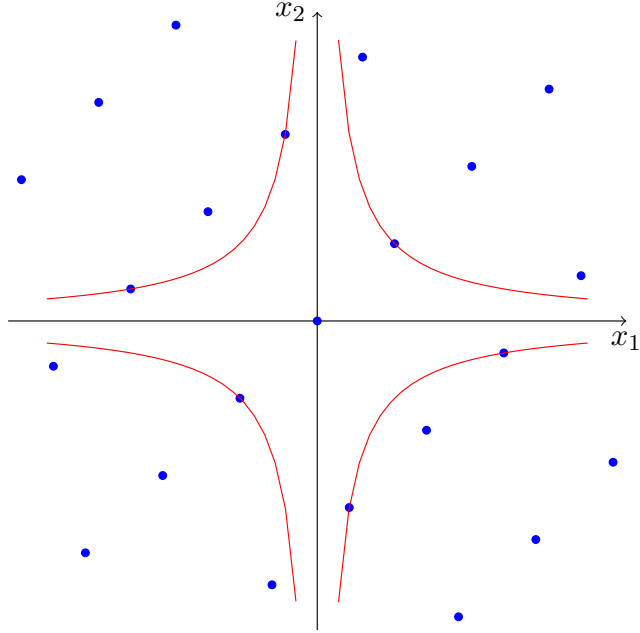
Figure 2: Admissible lattice and hyperbolic cross.

Crucial for the performance of the Frolov cubature formula (1.9) will be the notion of "admissibility" which is settled in the following definition.

Definition 2.7 (Admissible lattice). *A lattice Γ is called admissible if*

$$\mathrm{Nm}(\Gamma) := \inf_{\gamma \in \Gamma \setminus \{0\}} \left| \prod_{i=1}^{d} \gamma_i \right| > 0 \tag{2.5}$$

holds true.

Figure 2 illustrates this property. In fact, lattice points different from 0 lie outside of a hyperbolic cross with "radius" $\mathrm{Nm}(\Gamma)$. The following lemma is essentially [18, Lem. 3.1/2].

Lemma 2.8. *If a lattice $\Gamma \subset \mathbb{R}^d$ is admissible then $\Gamma^\perp \subset \mathbb{R}^d$ is also admissible.*

The proof in [18] of this result uses the theory of geometry of numbers and is not constructive, i.e. we do not know the value of $\mathrm{Nm}(\Gamma^\perp)$. In the next section, we consider a more precise statement for Vandermonde-type lattices and therefore omit the proof here.

3 Construction of Vandermonde-type lattices

There is a generic way to construct an admissible lattice, for example described by Temlyakov [21, IV.4]. We will now introduce this construction using number field theory following the presentations in [15] and [9].

A *number field* is a subfield of $\mathbb{C}$ having finite degree as a field extension over $\mathbb{Q}$. Every such field can be expressed by $\mathbb{Q}(\alpha)$ for a suitable algebraic number $\alpha \in \mathbb{C}$. Let

$$p(x) = x^d + a_{d-1}x^{d-1} + \ldots + a_1 x + a_0 \in \mathbb{Q}[x] \tag{3.1}$$

be the unique monic polynomial of minimal order d satisfying $p(\alpha) = 0$. Then d is the degree of $\mathbb{Q}(\alpha)/\mathbb{Q}$, and we also call it the degree of α. We are interested in *algebraic integers*, which are algebraic numbers satisfying that the associated minimal polynomial has coefficients in $\mathbb{Z}$. All algebraic integers in $\mathbb{C}$ form a ring; to show this, we discuss an alternative characterization of algebraic integers.

Lemma 3.1. *An algebraic number $\alpha \in \mathbb{C}$ is an algebraic integer if and only if $\alpha \in R$ for some subring of $R \subset \mathbb{C}$ having a finitely generated additive group.*

Proof. Suppose α is an algebraic integer of order d. Then $\mathbb{Z}[\alpha]$ is a subring of $\mathbb{C}$ which is generated by $1, \alpha, \ldots, \alpha^{d-1}$. Now we assume that $\alpha \in R$ for some finitely generated subring $R \in \mathbb{C}$. We denote by $r_1, \ldots, r_n$ the generators of R, and express the numbers αr_i as a linear combination of the generators. This leads to the linear system

$$\alpha \begin{pmatrix} r_1 \\ \vdots \\ r_n \end{pmatrix} = M \begin{pmatrix} r_1 \\ \vdots \\ r_n \end{pmatrix},$$

where M is a $n \times n$-matrix with entries in $\mathbb{Z}$. We have that $r = (r_1, \ldots, r_n)^\top$ is an eigenvector of M with eigenvalue α, and therefore the determinant of $(\alpha I - M)$ is zero. If we expand

$$\det(\alpha I - M) = \alpha^n + \text{lower degree terms} = 0$$

we can see that α is a root of some monic polynomial $q(x) \in \mathbb{Z}[x]$. This implies that α is an algebraic number, with associated minimal polynomial $p(x) \in \mathbb{Q}[x]$.

It remains to show that $p(x)$ has integer coefficients. To this end, we write $q(x) = p(x)s(x)$, with a monic polynomial $s(x) \in \mathbb{Q}[x]$. Additionally define $k, l \in \mathbb{N}$ as the smallest integers such that $kp(x), ls(x) \in \mathbb{Z}[x]$. It follows that the coefficients of $kp(x)$ have no common divisor, same for $ls(x)$. If we assume that $kl > 1$, there exists a prime divisor m of kl, and in turn we have

$$0 = klq(x) = kp(x)ls(x) \in \mathbb{Z}_m[x].$$

Since $Z_m[x]$ is an integral domain, either $kp(x)$ or $ls(x)$ vanish in $Z_m[x]$. Therefore, either all coefficients of $kp(x)$ or $ls(x)$ are divisible by m, which is a contradiction. We conclude $kl = 1$, and subsequently $p(x) \in \mathbb{Z}[x]$. $\square$

Corollary 3.2. *For a number field K, the set of algebraic integers in K form a ring.*

Proof. Let $\alpha, \beta \in K$ be algebraic integers. Then

$$
\begin{aligned}
\alpha + \beta &\in \mathbb{Z}[\alpha, \beta], \\
\alpha\beta &\in \mathbb{Z}[\alpha, \beta].
\end{aligned}
$$

Since $\mathbb{Z}[\alpha]$ and $\mathbb{Z}[\beta]$ are finitely generated, so is $\mathbb{Z}[\alpha, \beta]$. $\square$

We now turn our attention to the different embeddings of a number field K of degree d into $\mathbb{C}$. For $K = \mathbb{Q}(\alpha)$ for some α and p its minimal polynomial, we have that p is irreducible over $\mathbb{Q}$ and therefore has d different roots $\alpha = \alpha_1, \ldots, \alpha_d$, which are called conjugates. Every field homomorphism $f : K \longrightarrow \mathbb{C}$ necessarily satisfies $p(f(\alpha)) = 0$, which implies that $f(\alpha) = \beta$ for a conjugate $\beta \in \{\alpha_1, \ldots, \alpha_d\}$, and consequently $f(g(\alpha)) = g(\beta)$ for all $g \in \mathbb{Q}[x]$. This means that there are exactly d different embeddings $K \hookrightarrow \mathbb{C}$. The following theorem describes the core property of algebraic numbers in the context of admissible lattices.

Theorem 3.3. *Let K be a number field of degree d and $\theta_1, \ldots, \theta_d$ be its distinct embeddings into $\mathbb{C}$. For any algebraic integer $\beta \in K \setminus \{0\}$ one has*

$$
\prod_{k=1}^{n} \theta_k(\beta) \in \mathbb{Z} \setminus \{0\}. \tag{3.2}
$$

Proof. Since for every $\beta \in \mathbb{Q}(\alpha)$ the field extension can be split into $\mathbb{Q}(\beta)/\mathbb{Q}$ and $\mathbb{Q}(\alpha)/\mathbb{Q}(\beta)$, the dimension formula immediately implies that the degree of β is a divisor of d. The degree of β will be called $b \in \mathbb{N}$, and let $c \in \mathbb{N}$ satisfy $bc = d$. Let $\psi_1, \ldots, \psi_b$ be the distinct embeddings of $\mathbb{Q}(\beta)$ into $\mathbb{C}$. We know that the minimal polynomial q of β has coefficients in $\mathbb{Z}$, and therefore

$$
\prod_{i=1}^{b} \psi_i(\beta) = \prod_{i=1}^{b} \beta_i \in \mathbb{Z} \setminus \{0\},
$$

where $\beta_1, \ldots, \beta_b$ are the roots of q. Moreover, every embedding ψ_i extends naturally to c distinct embeddings $\psi_{i1}, \ldots, \psi_{ic}$ from K into $\mathbb{C}$. The collection $\{\psi_{ij}\}_{i,j=1}^{b,c}$ equals $\{\theta_k\}_{k=1}^{d}$ and we finally obtain

$$
\prod_{k=1}^{d} \theta_i(\beta) = \prod_{j=1}^{c} \prod_{i=1}^{b} \psi_{ij}(\beta) = \left(\prod_{i=1}^{b} \psi_i(\beta) \right)^c \in \mathbb{Z} \setminus \{0\}. \qquad \square
$$

We now present the standard construction of admissible lattices using the introduced theory, in the form of a corollary.

Corollary 3.4. *Let $p(x)$ be a polynomial of degree d satisfying*

- *p has integer coefficients,*

- *p has leading coefficient 1,*

- *p is irreducible over $\mathbb{Q}$,*

- *p has d different real roots $\xi_1, \ldots, \xi_d$.*

The Vandermonde matrix

$$A = \begin{pmatrix} 1 & \xi_1 & \cdots & \xi_1^{d-1} \\ 1 & \xi_2 & \cdots & \xi_2^{d-1} \\ \vdots & \vdots & \ddots & \vdots \\ 1 & \xi_d & \cdots & \xi_d^{d-1} \end{pmatrix} \in GL_d(\mathbb{R}) \tag{3.3}$$

generates an admissible lattice $\Gamma = A(\mathbb{Z}^d)$ with $\mathrm{Nm}(\Gamma) = 1$ and determinant

$$\det(\Gamma) = \prod_{k<l} |\xi_k - \xi_l| \,. \tag{3.4}$$

Proof. Let $m \in \mathbb{Z}^d$, and $p_m(x) = m_1 + m_2 x + \ldots + m_d x^{d-1}$ be the corresponding polynomial. Since ξ_1 is an algebraic integer in $\mathbb{Q}(\xi_1)$, so is $p_m(\xi_1)$, which follows from the ring structure of algebraic integers. Defining the field homomorphisms $\theta_1, \ldots, \theta_d$ via

$$\theta_i(\xi_1) = \xi_i \,, \quad i = 1, \ldots, d \,,$$

(which are the d distinct embeddings from $\mathbb{Q}(\xi_1)$ into $\mathbb{C}$) one has

$$\prod_{i=1}^d (Am)_i = \prod_{i=1}^d p_m(\xi_i) = \prod_{i=1}^d \theta_i(p_m(\xi_1)) \in \mathbb{Z} \setminus \{0\} \,,$$

as shown in Theorem 3.3. This implies $\mathrm{Nm}(\Gamma) \geq 1$; equality is attained for $m = (1, 0, \ldots, 0)^\top$. Finally, the formula for the determinant of Γ follows directly from the Vandermonde structure of A. $\qquad\square$

It is important to note that a small determinant (3.4) will be favorable for the convergence behavior of the Frolov cubature formula (1.9) (see Section 6). We end this section with a property of Vandermonde-type lattices regarding the norm of the dual lattice.

Theorem 3.5. *Let A and $\Gamma = A(\mathbb{Z}^d)$ be as in Corollary 3.4. Then the equation*

$$\frac{\mathrm{Nm}(\Gamma)}{\det(\Gamma)} = \frac{\mathrm{Nm}(\Gamma^\perp)}{\det(\Gamma^\perp)} \, , \tag{3.5}$$

holds.

Proof. The lattice $\Gamma^\perp$ is generated by $A^{-\top}$. Using the Hankel-decomposition for Vandermonde matrices [14] of $A^{-\top} = DAH$ with a diagonal matrix D satisfying $\det(D) = \det(A)^{-2} = \det(\Gamma)^{-2}$ and H unimodular, we obtain

$$\mathrm{Nm}(\Gamma^\perp) = \mathrm{Nm}(DAH(\mathbb{Z}^d)) = \frac{\mathrm{Nm}(A(\mathbb{Z}^d))}{\det(\Gamma)^2} = \frac{\mathrm{Nm}(\Gamma)}{\det(\Gamma)^2} \, ,$$

which gives the result since $\det(\Gamma)^{-1} = \det(\Gamma^\perp)$. $\qquad\square$

This theorem shows that for Vandermonde-type lattices, the norm form $\mathrm{Nm}(\cdot)$ behaves well under the duality operation.

Remark 3.6. *One can ask if* (3.5) *holds true for general lattices Γ. We could not find any results in the literature concerning this question. Sadly, the proof in [18] showing the admissibility of the dual lattice is not constructive.*

4   The Chebyshev lattice

In this section we deal with scaled Chebyshev polynomials and the corresponding lattices obtained from Corollary 3.4.

The usual Chebyshev polynomials (of the first kind) $T_d(x)$ are defined via the recurrence relation

$$T_0(x) = 1\,, \tag{4.1}$$

$$T_1(x) = x\,, \tag{4.2}$$

$$T_d(x) = 2xT_{d-1}(x) - T_{d-2}(x)\,. \tag{4.3}$$

It is easy to see that the d-th Chebyshev polynomial has order d and its coefficients are integers. However, it cannot be used for Corollary 3.4 since the leading coefficient is not 1 for $d > 1$. In fact, writing

$$T_d(x) = a_d x^d + a_{d-1} x^{d-1} + \ldots + a_1 x + a_0 \tag{4.4}$$

for $d > 0$ it is easy to see that a_i is divisible by 2^{i-1}. Therefore, the scaled Chebyshev polynomials

$$Q_d(x) = 2T_d(x/2)\,, \quad d \in \mathbb{N}\,, \tag{4.5}$$

still have integer coefficients, and in addition the leading coefficient is 1. Concerning the roots of $Q_d(x)$, consider the equivalent definition of the Chebyshev polynomials

$$T_d(x) = \cos(d \arccos(x)) \tag{4.6}$$

which is explicit. The roots of $T_d(x)$ are then given by

$$\tau_k = \cos\left(\pi \frac{2k-1}{2d}\right)\,, \quad k = 1, \ldots, d\,, \tag{4.7}$$

and this implies that the roots of $Q_d(x)$ are

$$\xi_k = 2\tau_k = 2\cos\left(\pi \frac{2k-1}{2d}\right)\,, \quad k = 1, \ldots, d\,. \tag{4.8}$$

These roots are real-valued and pairwise different. Therefore Corollary 3.4 (ignoring the irreducibility condition for now) can be used to obtain the Vandermonde matrix T with

$$T_{kl} = \begin{cases} 1 & l = 1\,, \\ \left(2\cos\left(\pi \frac{2k-1}{2d}\right)\right)^{l-1} & l = 2, \ldots, d\,. \end{cases} \tag{4.9}$$

The corresponding lattice $T(\mathbb{Z}^d)$ we call *Chebyshev lattice*. The main result of this section reads as follows.

Theorem 4.1. *The Chebyshev lattice $\Gamma_T = T(\mathbb{Z}^d)$ is an orthogonal lattice.*

To show this, a lattice representation $\tilde{T} = TS$, $S \in \mathrm{SL}_d(\mathbb{Z})$ will be introduced, and subsequently will be proven to have orthogonal column vectors.

Lemma 4.2. *For $\omega \in \mathbb{R}$ and $l \in \mathbb{N}$ define $\eta_l = 2\cos(l\omega\pi)$. Then*

$$\eta_1^l - \eta_l \in \mathbb{Z}[\eta_1, \ldots, \eta_{l-1}] \quad , \quad l \in \mathbb{N}.$$

More precisely, there exist integers $m_j^{(l)} \in \mathbb{Z}$ independent of ω such that for any $l \in \mathbb{N}$

$$\eta_1^l - \eta_l = m_0 + \sum_{j=1}^{l-1} m_j^{(l)} \eta_j \,.$$

Proof. The proof is a straightforward calculation using Euler's formula by putting

$$
\begin{aligned}
\eta_1^l - \eta_l &= \left(e^{\omega\pi\mathrm{i}} + e^{-\omega\pi\mathrm{i}} \right)^l - \left(e^{\omega\pi\mathrm{i}l} + e^{-\omega\pi\mathrm{i}l} \right) \\
&= \sum_{j=0}^{l} \binom{l}{j} e^{\omega\pi\mathrm{i}(l-2j)} - \left(e^{\omega\pi\mathrm{i}l} + e^{-\omega\pi\mathrm{i}l} \right) \\
&= \sum_{j=1}^{l-1} \binom{l}{j} e^{\omega\pi\mathrm{i}(l-2j)} \\
&= \begin{cases} \displaystyle\sum_{j=1}^{\frac{l-1}{2}} \binom{l}{j} \left(e^{\omega\pi\mathrm{i}(l-2j)} + e^{-\omega\pi\mathrm{i}(l-2j)} \right) & l \text{ odd}, \\[2em] \displaystyle\sum_{j=1}^{\lfloor\frac{l-1}{2}\rfloor} \binom{l}{j} \left(e^{\omega\pi\mathrm{i}(l-2j)} + e^{-\omega\pi\mathrm{i}(l-2j)} \right) + \binom{l}{\frac{l}{2}} e^{\omega\pi\mathrm{i}(l-l)} & l \text{ even} \end{cases} \\
&= \begin{cases} \displaystyle\sum_{j=1}^{\frac{l-1}{2}} \binom{l}{j} 2\cos(\omega\pi(l-2j)) & l \text{ odd}, \\[2em] \displaystyle\sum_{j=1}^{\lfloor\frac{l-1}{2}\rfloor} \binom{l}{j} 2\cos(\omega\pi(l-2j)) + \binom{l}{\frac{l}{2}} & l \text{ even}. \end{cases}
\end{aligned}
$$

The values $m_j^{(l)}$ can be obtained from this representation. $\qquad\square$

This lemma leads to the desired lattice representation, since multiplying with a matrix $S \in \mathrm{SL}_d(\mathbb{Z})$ from the right is a composition of column operations.

Corollary 4.3. *The matrix* $\tilde{T} = TS$ *given by*

$$\tilde{T}_{kl} = \begin{cases} 1 & l = 1, \\ 2\cos\left(\pi(l-1)\frac{2k-1}{2d}\right) & l = 2, \ldots, d, \end{cases} \tag{4.10}$$

where $S \in SL_d(\mathbb{Z})$ *is a suitable column operation matrix, generates the lattice* $\Gamma_T = T(\mathbb{Z}^d)$.

Proof. The case $d = 2$ is trivial, so let $d > 2$. For $l = 3, \ldots, d$ we define $S^{(l)} \in \mathrm{SL}_d(\mathbb{Z})$ to be a column operation matrix changing the l-th column:

$$S^{(l)} = \begin{pmatrix} 1 & & & -m_0^{(l)} & & \\ & \ddots & & \vdots & & \\ & & \ddots & -m_{l-2}^{(l)} & & \\ & & & 1 & & \\ & & & & \ddots & \\ & & & & & 1 \end{pmatrix}. \tag{4.11}$$

Then the product matrix $S = S^{(3)} \cdots S^{(d)}$ consecutively transforms the entries of T which have the form $\xi_k^{l-1} = 2\cos(\pi \frac{2k-1}{2d})^{l-1}$ according to Lemma 3.2. $\qquad\square$

We remark that this formula is applicable in general to any Vandermonde-type lattice with generating factors ranging from -2 to 2, which in this case are the Chebyshev roots $\xi_1, \ldots, \xi_d$. Furthermore, $\tilde{T}$ is given explicitly. This bypasses stability issues appearing in the context of Vandermonde matrices, and solves the problem of finding a proper lattice representation for the Chebyshev lattices. The following lemma will complete the proof of Theorem 4.1.

Lemma 4.4. *The matrix* $\tilde{T}$ *is orthogonal. Moreover, it holds that* $\tilde{T}^\top \tilde{T} = \mathrm{diag}(d, 2d, ..., 2d)$.

Proof. For $l = 2, \ldots, d$ one has

$$\begin{aligned} ((\tilde{T})^\top \tilde{T})_{1l} &= \sum_{k=1}^{d} 2\cos\left(\pi(l-1)\frac{2k-1}{2d}\right) \\ &= \sum_{k=1}^{d} \left(e^{i\pi(l-1)\frac{2k-1}{2d}} + e^{-i\pi(l-1)\frac{2k-1}{2d}}\right) \\ &= \sum_{k=1}^{2d} e^{i\pi(l-1)\frac{2k-1}{2d}}. \end{aligned}$$

Furthermore, one finds

$$\sum_{k=1}^{2d} e^{2\pi i(l-1)\frac{2k-1}{4d}} = \left(\sum_{k=1}^{2d} e^{2\pi i(l-1)\frac{k}{2d}}\right) e^{\frac{-2\pi i(l-1)}{4d}} = \frac{1 - e^{2\pi i(l-1)}}{1 - e^{2\pi i\frac{(l-1)}{2d}}} e^{\frac{-2\pi i(l-1)}{4d}} = 0\,.$$

The case of $l = 2, \ldots, d$ and $j = 2, \ldots, d$ is treated similarly:

$$
\begin{aligned}
((\tilde{T})^\top \tilde{T})_{jl} &= \sum_{k=1}^{d} 2\cos\left(\pi(j-1)\frac{2k-1}{2d}\right) 2\cos\left(\pi(l-1)\frac{2k-1}{2d}\right) \\
&= \sum_{k=1}^{d} \left(e^{\pi i(j-1)\frac{2k-1}{2d}} + e^{-\pi i(j-1)\frac{2k-1}{2d}}\right)\left(e^{\pi i(l-1)\frac{2k-1}{2d}} + e^{-\pi i(l-1)\frac{2k-1}{2d}}\right) \\
&= \sum_{k=1}^{d} e^{\pi i(j+l-2)\frac{2k-1}{2d}} + e^{\pi i(j-l)\frac{2k-1}{2d}} + e^{\pi i(l-j)\frac{2k-1}{2d}} + e^{-\pi i(j+l-2)\frac{2k-1}{2d}} \\
&= \sum_{k=1}^{2d} e^{2\pi i(j+l-2)\frac{2k-1}{4d}} + \sum_{k=1}^{2d} e^{2\pi i(j-l)\frac{2k-1}{4d}} = \begin{cases} 2d & j = l\,, \\ 0 & \text{otherwise}\,. \quad \square \end{cases}
\end{aligned}
$$

We now return to the issue concerning the irreducibility of $Q_d(x)$ over $\mathbb{Q}$.

Lemma 4.5. *The polynomial $Q_d(x)$ is irreducible over $\mathbb{Q}$ if and only if $d = 2^m$ for some $m \in \mathbb{N}_0$.*

Proof. It has been shown in for instance [21, p. 242] that $Q_d(x)$ is irreducible for $d = 2^m$. This is done in the following way: First we see that

$$Q_{2^m}(x) = Q_{2^{m-1}}(x)^2 - 2$$

holds for $m \in \mathbb{N}$, using (4.6) and the formula $\cos(2x) = 2\cos(x)^2 - 1$. This implies that the coefficients a_n of $Q_{2^m}(x) = \sum_{n=0}^{2^m} a_n x^n$ are even if $n < 2^m$. Assuming that $Q_{2^m}(x)$ is reducible, we can write it as a product of two monic polynomials

$$Q_{2^m}(x) = p(x)q(x) = \left(\sum_{u=0}^{s} p_u x^u\right)\left(\sum_{v=0}^{t} q_v x^v\right)$$

which have integer coefficients (cf. the proof of Lemma 3.1). It is easy to see that $|a_0| = |p_0 q_0| = 2$, thus w.l.o.g p_0 is even and q_0 is odd. Using the formulas

$$a_n = \sum_{\substack{u+v=n \\ u \le s \\ v \le t}} p_u q_v\,, \quad n \le d\,,$$

one can show inductively that p_u is even for all $u = 0, \ldots, s$. This is a contradiction, since $p(x)$ is a monic polynomial.

16

Now let $d \in \mathbb{N}$ have a divisor not equal to 2. We decompose $d = d'p$ such that p is not divisible by 2, and define $q_i = (2i - 1)p, i = 1, \ldots, d'$. Since q_i is an odd number smaller than $2d$, $k_i = \frac{m_i + 1}{2}$ is a natural number smaller than d. The polynomial

$$
\begin{aligned}
\prod_{i=1}^{d'} (x - \xi_{k_i}) &= \prod_{i=1}^{d'} \left[x - 2\cos\left(\pi \frac{2k_i - 1}{2d} \right) \right] \\
&= \prod_{i=1}^{d'} \left[x - 2\cos\left(\pi \frac{q_i}{2d} \right) \right] \\
&= \prod_{i=1}^{d'} \left[x - 2\cos\left(\pi \frac{(2i - 1)p}{2d} \right) \right] \\
&= \prod_{i=1}^{d'} \left[x - 2\cos\left(\pi \frac{(2i - 1)}{2d'} \right) \right] \\
&= Q_{d'}(x)
\end{aligned}
$$

is an element of $\mathbb{Z}[x]$ and a divisor of $Q_d(x)$. $\qquad \square$

This means that we can use $Q_d(x)$ to construct an admissible lattice if and only if $d = 2^m$ for some $m \in \mathbb{N}_0$. In this case, we call the resulting lattice Γ *Chebyshev-Frolov lattice*.

5   Enumeration of the Frolov points

In this section we deal with the problem of enumerating the set $X = \Gamma \cap \Omega$ for a d-dimensional lattice Γ and the integration domain $\Omega = [-1/2, 1/2]^d$. This is a necessary preprocessing step for the implementation of the Frolov cubature formula (1.9). To make Γ accessible to a computer, we need to specify a lattice representation matrix $A \in \mathrm{GL}_d(\mathbb{R})$ such that $\Gamma = A(\mathbb{Z}^d)$. It is an equivalent problem to determine the set $Y = \mathbb{Z}^d \cap (A^{-1}\Omega)$, and the complexity of this task will strongly depend on the choice of A.

Bounding set strategy. The main idea of the following algorithms is simple: We define a larger set $Y \subset \mathbf{Y} \subset \mathbb{Z}^d$ which allows for an easy enumeration. More precisely, the set $\mathbf{Y} = \mathbf{Y}(d, p) \subset \mathbb{Z}^d$ should satisfy an axis-aligned recursive representation formula

$$\mathbf{Y}(j, p) = \bigcup_{k_j \in K_{j-1}(p)} \mathbf{Y}(j-1, f_{j-1}(p, k_j)) \times \{k_j\}, \, j = 1, \ldots, d \tag{5.1}$$

where $\mathbf{Y}(0, f_0(p, k_1)) := k_1$, p stands for a set of parameters describing the size of $\mathbf{Y}$ and the functions $f_1, \ldots, f_{d-1}$ determine the local dependence on the components k_j and p. $K_j(p) \subset \mathbb{Z}$ is a bounded set of the form $\{k \in \mathbb{Z} : a_j(p) \le k \le b_j(p)\}$. For simplicity, we will assume that these sets always contain 0, which will also be the case for all subsequent examples. We can define a recursive algorithm which iterates over the elements $y \in \mathbf{Y}$ and checks if $y \in Y$, outlined in Algorithm 1. The complexity of this algorithm will always be linearly dependent on the cardinality of the corresponding bounding set, and therefore we will identify the complexity of Algorithm 1 with the cardinality of the bounding set in use. In the following, we present two suitable bounding sets: the bounding box and the bounding ellipsoid.

Bounding box. We consider the axis-parallel cuboid with corresponding widths $r_1, \ldots, r_d > 0$

$$C_r = \{x \in \mathbb{R}^d : |x_i| \le r_i, i = 1, \ldots, d\} \tag{5.2}$$

and ask whether $A^{-1}\Omega \subset C_r$ holds. A simple calculation shows that

$$
\begin{aligned}
A^{-1}\Omega &\subset C_r \\
\Leftrightarrow A^{-1}[-1/2, 1/2]^d &\subset C_r \\
\Leftrightarrow \frac{1}{2}|A^{-\top}e_i|_1 &\le r_i, \quad i = 1, \ldots, d,
\end{aligned}
$$

where $e_1, \ldots, e_d$ form the standard basis of $\mathbb{R}^d$. This allows us to set $r_i = \frac{1}{2}|A^{-\top}e_i|_1$ and define the bounding box with parameters $p = \{r_i\}_{i=1}^d$

$$\mathbf{Y} = \mathbf{Y}_{\mathrm{Box}}(d, p) = \{k \in \mathbb{Z}^d : |k_i| \le r_i, i = 1, \ldots, d\} = C_r \cap \mathbb{Z}^d, \tag{5.3}$$

which obviously satisfies (5.1) for the functions $f_{j-1}(p, k_j) = p$ and the sets $K_{j-1}(p) = \{k \in \mathbb{Z} : |k| \le r_j\}$ (cf. Figure 5). The number of points in $\mathbf{Y}_{\mathrm{Box}}$ is given by

$$|\mathbf{Y}_{\mathrm{Box}}| = \prod_{i=1}^d (2\lfloor r_i \rfloor + 1) = \prod_{i=1}^d \left(2\left\lfloor \frac{1}{2}|A^{-\top}e_i|_1 \right\rfloor + 1\right). \tag{5.4}$$

18

Algorithm 1: Assemblation of the set $Y = \mathbb{Z}^d \cap (A^{-1}\Omega)$.

Input:

Integration domain Ω,

Lattice representation A,

Covering set **Y** with recursive structure (5.1),

initial parameters p_{init}

---

set $Y = \emptyset$

run `assemble` $(Y, d, p_{init}, 0)$

Function `assemble` $(Y, j, p, (m_i)_{i=1}^d)$

    if $j \geq 2$ **then**

        forall $k_j \in K_{j-1}(p)$ **do**

            set $m_j = k_j$

            `assemble` $(Y, j - 1, f_{j-1}(p, k_j), m)$

    if $j = 1$ **then**

        forall $k_1 \in K_0(p)$ **do**

            set $m_1 = k_1$

            if $Am \in \Omega$ **then**

                set $Y = Y \cup \{m\}$

Output: Set of lattice points Y

The choice of A is crucial here; Figure 3 shows the sets AC_r for different lattice representations.

Bounding ellipsoid. Now, we assume that the lattice $\Gamma = A(\mathbb{Z}^d)$ is orthogonal, i.e. A has orthogonal column vectors. We further decompose $A = QD$ into an orthonormal matrix Q with $Q^\top Q = I$ and a diagonal matrix $D = \operatorname{diag}(\lambda_1, \ldots, \lambda_d)$. Using the fact that an orthonormal matrix is a rotation, we can compute

$$
\begin{aligned}
Y &= \mathbb{Z}^d \cap (A^{-1}\Omega) = \mathbb{Z}^d \cap (D^{-1}Q^\top \Omega) \\
&\subset \mathbb{Z}^d \cap (D^{-1}Q^\top B_r^2(0)) = \mathbb{Z}^d \cap (D^{-1}B_r^2(0)) \\
&= \left\{ k \in \mathbb{Z}^d : \sum_{i=1}^d (\lambda_i k_i)^2 \leq r^2 \right\} =: \mathbf{Y}_{\mathrm{Ell}}(d, r, \{\lambda_i\}_{i=1}^d),
\end{aligned}
$$

where $B_r^2(0)$ is the Euclidean ball centered at 0 with radius $r = \sqrt{d}/2$, chosen such that $\Omega \subset B_r^2(0)$, see also Figure 4. The sets $\mathbf{Y}_{\mathrm{Ell}} = \mathbf{Y}_{\mathrm{Ell}}(j, r, p)$ are axis-aligned ellipsoids and therefore satisfy the recursion formula (5.1)(see Figure 5). Algorithm 1 is applicable by choosing $p = \{\lambda_i\}_{i=1}^d$, the functions $f_{j-1}(r, p, k_j) = \left(\sqrt{r^2 - (\lambda_j k_j)^2}, p \right)$, and $K_{j-1}(r, p) =$
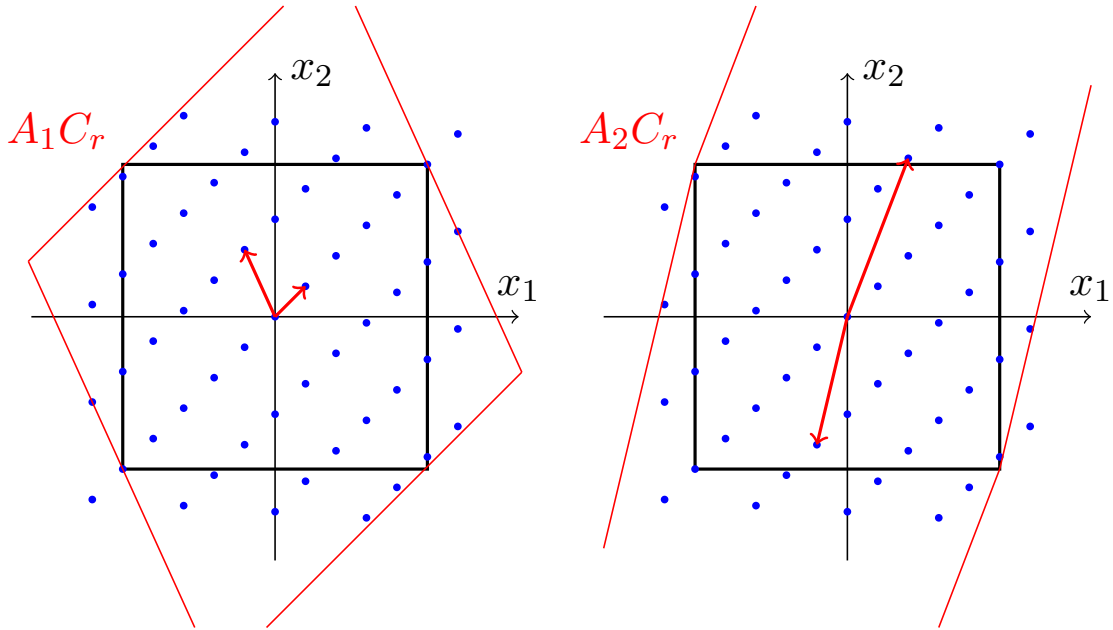
Figure 3: The sets AC_r for different lattice representations A_1 and A_2.
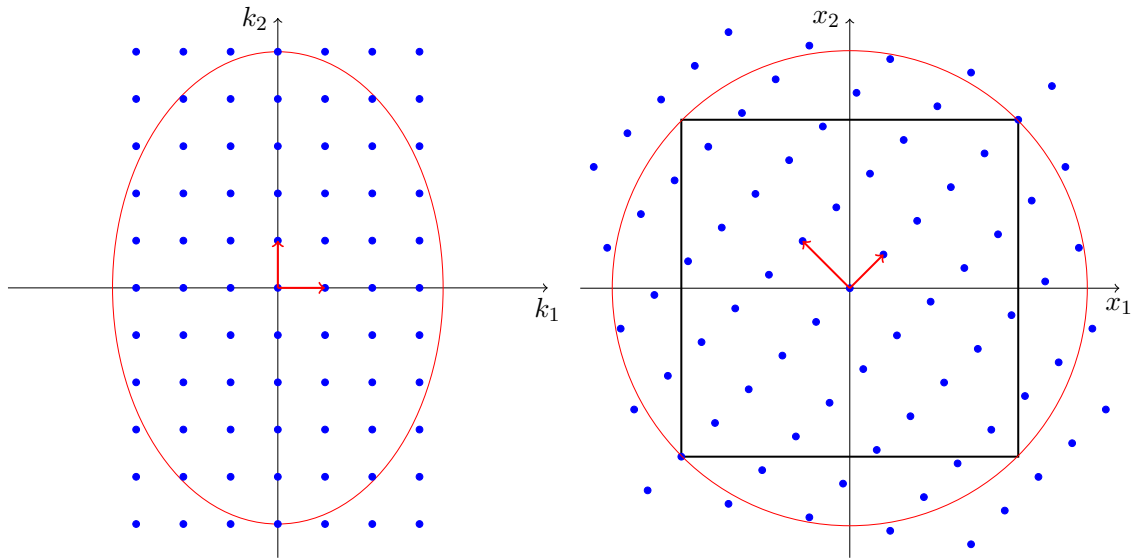
Figure 4: The ellipsoid (left) that is the pre-image under A of the bounding ball $B_r^2(0)$ of $\Omega = [-1/2, 1/2]^2$ (right).
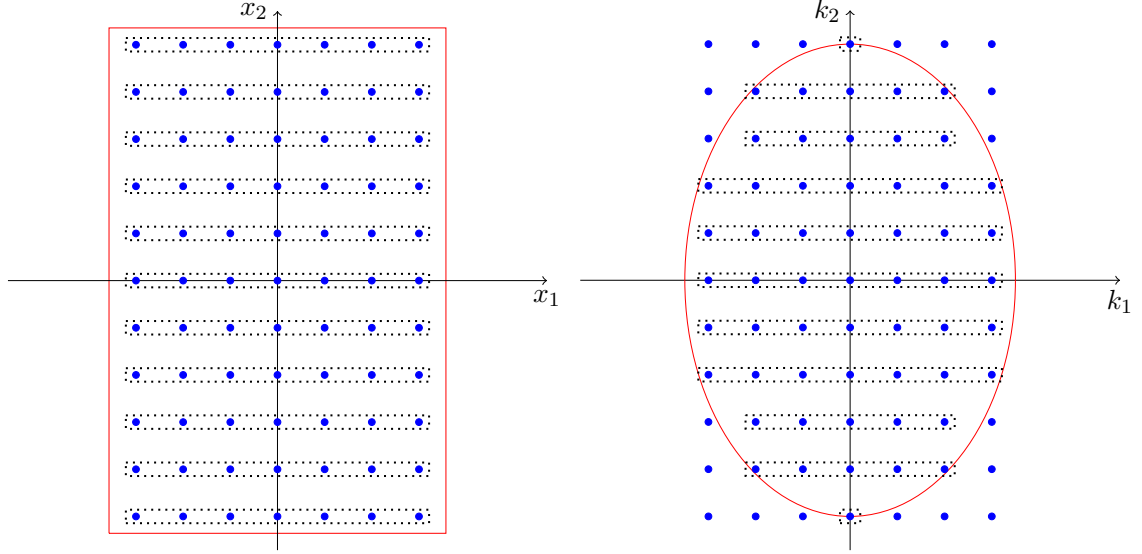
Figure 5: Recursive grouping of the sets $\mathbf{Y}_{\mathrm{Box}}$ (left) and $\mathbf{Y}_{\mathrm{Ell}}$ (right) in two dimensions.

$\{k \in \mathbb{Z} : |k| \leq r/\lambda_j\}$. The cardinality of $\mathbf{Y}_{\mathrm{Ell}}$ can only be estimated; we will discuss it later in this section.

Further reduction. Algorithm 1 can be accelerated if certain conditions are satisfied. We will heavily rely on the special geometry of $\Omega = [-1/2, 1/2]^d$, especially on the fact that it is convex. We start with a covering set $\mathbf{Y}$ satisfying a recursive formula (5.1). Let $j < d$ be a positive integer, and $(k_{j+1}, \ldots, k_d)^\top \in \mathbb{Z}^{d-j}$ be an integer vector such that

$$X = \mathbf{Y}(j, p) \times \{(k_{j+1}, \ldots, k_d)^\top\} \subset \mathbf{Y} \tag{5.5}$$

for some parameters p, i.e. Algorithm 1 iterates over X at some point. Then it may be the case that $X \cap A^{-1}\Omega = \emptyset$. Knowing this beforehand, one could of course accelerate the algorithm by leaving X out. We will use this idea, capitalizing on the special geometry of $\Omega = [-1/2, 1/2]^d$ and on a property all lattices Γ coming from Corollary 3.4 (and scaled versions) have:

$$v = c \cdot (1, \ldots, 1)^\top \in \Gamma \tag{5.6}$$

for some $c > 0$, and we choose it to be $c = \min\{c > 0 : v \in \Gamma\}$. A useful function in this context is

$$h(x) = \max_{i=1,\ldots,d} x_i - \min_{i=1,\ldots,d} x_i \tag{5.7}$$

because it satisfies $h(x + av) = h(x)$ for any $a \in \mathbb{R}$. Additionally, $h(x) \leq 1$ for all $x \in \Omega$. If we impose on the lattice representation A that its first column vector is v, it is now easy to

see that

$$h(A(0, k_2, \ldots, k_d)^\top) > 1 \tag{5.8}$$
$$\Rightarrow \mathbf{Y}(1, p) \times \{(k_2, \ldots, k_d)\} \cap A^{-1}\Omega = \emptyset.$$

This can be generalized, because $h(x + y) \geq h(x) - h(y)$ holds for all $x, y \in \mathbb{R}^d$. Let $A = (v|a_2|\ldots|a_d)$, then

$$h(A(0, \ldots, 0, k_{j+1}, \ldots, k_d)^\top) - \sum_{i=2}^{j} b_i h(a_i) > 1 \tag{5.9}$$
$$\Rightarrow X = \mathbf{Y}(j, p) \times \{(k_{j+1}, \ldots, k_d)\} \cap A^{-1}\Omega = \emptyset,$$

where the parameters b_i have to be determined accordingly, using the specific recursive structure $\mathbf{Y}$ has. For the bounding box approach one can take $b_i = \lfloor r_i \rfloor$, for the bounding ellipsoid sets $\mathbf{Y}_{\mathrm{Ell}}(j, r, \{\lambda_1, \ldots, \lambda_j\})$ it is appropriate to take $b_i = \lfloor r/\lambda_i \rfloor$. Implementing this as a break condition in Algorithm 1 leads to a significant reduction of the complexity. We model the complexity of this reduction applied to the bounding ellipsoid approach, defining the function

$$H_l(\mathbf{Y}_{\mathrm{Ell}}(j, p) \times \{(k_{j+1}, \ldots, k_d)\}) = \begin{cases} (0, \ldots, 0, k_{j+1}, \ldots, k_d) & j \leq l \text{ and } (5.9), \\ \mathbf{Y}_{\mathrm{Ell}}(j, p) \times \{(k_{j+1}, \ldots, k_d)\} & \text{else}, \end{cases} \tag{5.10}$$

and then we obtain the new l-level bounding set $\mathbf{Y}_{\mathrm{Ell}}^l(d, p)$ via

$$\mathbf{Y}_{\mathrm{Ell}}^l(j, p) = \bigcup_{k_j \in K_{j-1}(p)} H_l\left(\mathbf{Y}_{\mathrm{Ell}}^l(j - 1, f_{j-1}(p, k_j)) \times \{k_j\}\right), j = 1, \ldots, d. \tag{5.11}$$

We set $H_l(\mathbf{Y}_{\mathrm{Ell}}(j, p) \times \{(k_{j+1}, \ldots, k_d)\})$ to its base point $(0, \ldots, 0, k_{j+1}, \ldots, k_d)$ to stay consistent with our complexity concept. The choice of l does matter, since the estimation used to derive (5.9) is far from strict for large j, which results in unnecessary additional computation time if one chooses $l = d$. We will use $l = m$ for $d = 2^m$, which proved to be effective in our simulations. We can optimize the algorithm even further, using the fact that $h(x)$ is convex. This is clear since the maximum function is convex and the minimum function is concave. Ω is convex too, which implies that the set

$$K'_{j-1}(p) = \{k \in K_{j-1}(p) : j > l \text{ or } (5.9) \text{ is false for } k = k_j\} \tag{5.12}$$

is also of the form $K'_{j-1}(p) = \{k \in \mathbb{Z} : a'_{j-1}(p) \leq k \leq b'_{j-1}(p)\}$. If this set contains 0, we can program our algorithm to iterate over $K'_{j-1}(p)$, starting at 0 and going in positive and negative direction. If it does not contain 0, one can check the slopes $h(x) - h(y)$ for $x = A(0, \ldots, 0, k_{j+1}, \ldots, k_d)^\top$ and $y = A(0, \ldots, 0, \pm 1, k_{j+1}, \ldots, k_d)^\top$. With this information, we can take the y for which $h(x) - h(y)$ is negative (if both slopes are positive, we return) and sharpen the estimate (5.9) by replacing $b_j h(a_j)$ with $b_j(h(x) - h(y))$. If the iteration is still valid, we go into the direction of descent until we brush over $K'_{j-1}(p)$ or we reach one

22

Algorithm 2: Assemblation of the set $Y = \mathbb{Z}^d \cap (A^{-1}\Omega)$.

Input:

Integration domain $\Omega = [-1/2, 1/2]^d$,

Lattice representation A with first column vector v as in (5.6),

Covering set $\mathbf{Y}^{*,l}_{\text{Ell}}$ with structure (5.14),

initial parameters $p_{init} = (r_{init}, \{\lambda_i\}^d_{i=1})$,

initial radius $r_{init} = \sqrt{d}/2$,

$f_{j-1}(p, k_j) = \left(\sqrt{r^2 - (\lambda_j k_j)^2}, p \right)$,

$K_{j-1}(p) = \{k \in \mathbb{Z} : |k| \leq r/\lambda_j\}$,

$b_j = \lfloor r/\lambda_j \rfloor$

$Y \leftarrow \emptyset$

run `assemble` $(Y, d, p_{init}, 0)$

Function `assemble` $(Y, j, p, (m_i)^d_{i=1})$

    if $j = 1$ **then**

        oneDimensionalAssemble(Y, m)

    if $1 < j \leq l$ **then**

        reducedAssemble$(Y, j, f_{j-1}(p, k_j), m)$

    if $j > l$ **then**

        trivialAssemble$(Y, j, f_{j-1}(p, k_j), m)$

Output: Set of lattice points Y

---

end of the set $K_{j-1}(p)$. Finally, we note that $K'_0(p)$ is easy to determine since (5.6) implies that for $x = (0, k_2, \ldots, k_d), h(x) < 1$ the point $z = x + sv \in \Gamma$,

$$s = - \left[\frac{1}{2c} \left(\max_{i=1,\ldots,d} x_i + \min_{i=1,\ldots,d} x_i \right) \right], \tag{5.13}$$

(where the brackets $[\cdot]$ denote the rounding operation in this case) has the lowest ℓ^∞-norm and therefore can serve as a starting point for the iteration over $K'_0(p)$ if $\|z\|_\infty < 0.5$. The reduced iteration set we denote with $K^*_{j-1}(p)$, and we get the further improved bounding set $\mathbf{Y}^{*,l}_{\text{Ell}}$ via

$$\mathbf{Y}^{*,l}_{\text{Ell}}(j, p) = \bigcup_{k_j \in K^*_{j-1}(p)} H_l \left(\mathbf{Y}^{*,l}_{\text{Ell}}(j - 1, f_{j-1}(p, k_j)) \times \{k_j\} \right), j = 1, \ldots, d. \tag{5.14}$$

The precise iteration over this set is summarized in Algorithm 2.

Complexity. We demonstrate the complexities of the respective methods using scaled versions of the Chebyshev-Frolov lattice Γ for dimensions $d \in \{2, 4, 8, 16\}$, together with the

---

Procedure oneDimensionalAssemble

Input:

integration point container Y,

base point $(m_i)_{i=1}^d$

---

if $h(Am) > 1$ **then return**

$m_1 \leftarrow s$ via (5.13)   `/* x + sv has the lowest ℓ∞-norm */`

while $\|Am\|_\infty < 0.5$ **do**

    $Y \leftarrow Y \cup \{m\}$

    $m_1 \leftarrow m_1 + 1$ `/* look for adjacent nodes in positive direction */`

$m_1 \leftarrow s - 1$ via (5.13)

while $\|Am\|_\infty < 0.5$ **do**

    $Y \leftarrow Y \cup \{m\}$

    $m_1 \leftarrow m_1 - 1$ `/* look for adjacent nodes in negative direction */`

Output: updated Y

Procedure reducedAssemble

Input:

integration point container Y,

level j,

parameters p,

base point $(m_i)_{i=1}^d$

$t \leftarrow h(Am) - \sum_{i=2}^{j-1} b_i h(a_i)$

$y_1 \leftarrow (0, \dots, 0, +1, m_{j+1}, \dots, m_d)$

$y_2 \leftarrow (0, \dots, 0, -1, m_{j+1}, \dots, m_d)$

$u \leftarrow \min\{h(Ay_1), h(Ay_2)\}$

if $u = h(Ay_1)$ **then**

    $q \leftarrow 1$

else

    $q \leftarrow -1$ `/* slope and descent direction */`

if $t - (h(Am) - u)b_j > 1 \wedge (h(Am) - u) > 0$ **then return**   `/* modified (5.9) */`

if $t > 1$ **then**

    if $h(Am) - u < 0$ **then return**   `/* positive slope */`

    $t_{old} \leftarrow t$

    while $\neg(t_{old} < 1 \wedge t > 1) \wedge m_j \leq b_j$ **do**   `/* brush over the valid set */`

        $m_j \leftarrow m_j + q$

        $t_{old} \leftarrow t$

        $t \leftarrow h(Am) - \sum_{i=2}^{j-1} b_i h(a_i)$

        if $t < 1$ **then** assemble $(Y, j-1, f_{j-1}(p, m_j), (m_i)_{i=1}^d)$

Output: updated Y

24

Procedure trivialAssemble

  Input:

  integration point container Y,

  level j,

  parameters p,

  base point $(m_i)_{i=1}^d$

---

  forall $k_j \in K_{j-1}(p)$ **do**   /* assemble as in Algorithm 1 */

     $m_j \leftarrow k_j$

     `assemble` $(Y, j-1, f_{j-1}(p, k_j), m)$

  Output: updated Y

---

orthogonal lattice representation obtained in Section 4. They are defined as

$$\Gamma_n = (\det(\Gamma)n)^{-1/d}\Gamma, \tag{5.15}$$

where $\Gamma = \tilde{T}(\mathbb{Z}^d)$ with $\tilde{T}$ as is Corollary 4.3, and n is the scaling parameter (Γ_n now has determinant $1/n$). The corresponding lattice representation is $\tilde{T}_n = (\det(\Gamma)n)^{-1/d}\tilde{T}$. We denote with $\mathbf{Y}_{\mathrm{Box}}(n)$ and $\mathbf{Y}_{\mathrm{Ell}}(n)$ the complexity of the bounding box approach and the bounding ellipsoid approach respectively, applied to the lattice Γ_n and the representation $\tilde{T}_n$. $\mathbf{Y}_{\mathrm{Ell}}^{*,l}(n)$ denotes the l-level reduced ellipsoid complexity, using ray search. Figure 6 and Figure 7 show the behavior of these quantities for increasing n.

The scaling parameter n and the number of integration points $N = N(n) = \Gamma_n \cap \Omega$ are related approximately by (see [18])

$$N = n + \mathcal{O}(\log^{d-1} n), \tag{5.16}$$

which explains the large difference of actual cubature points N and the scaling factor n for high dimensions and small n. The bounding box approach clearly has the highest complexity. In [11, Section 5] the complexity of the bounding ellipsoid approach was bounded from above and below:

Theorem 5.1. *Let* Γ_n, $\mathbf{Y}_{\mathrm{Ell}}(n)$ *and* N *be as above.*
(i) If $n > 2^{3d/2}$ *then the cardinality* $|\mathbf{Y}_{\mathrm{Ell}}(n)|$ *is bounded from below and above by*

$$n\left(1 - \frac{2^{3/2}}{n^{1/d}}\right)^d \frac{(d\pi)^{d/2}}{2^d\Gamma(d/2+1)} \quad \leq \quad |\mathbf{Y}_{\mathrm{Ell}}(n)| \quad \leq \quad n\left(1 + \frac{2^{3/2}}{n^{1/d}}\right)^d \frac{(d\pi)^{d/2}}{2^d\Gamma(d/2+1)}. \tag{5.17}$$

(ii) As a consequence, we obtain the limit statements

$$\lim_{n\to\infty} |\mathbf{Y}_{\mathrm{Ell}}(n)|/n = \lim_{n\to\infty} |\mathbf{Y}_{\mathrm{Ell}}(n)|/N = \mathrm{vol}((\sqrt{d}/2)B_2^d) \leq \left(\frac{\pi e}{2}\right)^{d/2} \approx 2.07^d. \tag{5.18}$$

This shows that the complexity of the bounding ellipsoid approach is linear in n, with a constant depending exponentially on d. The results of our simulation suggest that the specialized Algorithm 2 performs strictly better than Algorithm 1 using the bounding ellipsoid approach, which seems to converge to N for increasing n (cf. Figure 7). This would of course be the optimal behavior.

Dimension $d = 2$				
scaling factor n	integration points N	$\mathbf{Y}_{\mathrm{Box}}(n)$	$\mathbf{Y}_{\mathrm{Ell}}(n)$	$\mathbf{Y}_{\mathrm{Ell}}^{*,l}(n)$
64	65	165	101	83
256	257	609	409	295
1,024	1,027	2,337	1,599	1,105
4,096	4,095	9,315	6,427	4,249
16,384	16,383	36,869	25,735	16,689
65,536	65,539	$1.5 \cdot 10^5$	$1 \cdot 10^5$	66,149
262,144	262,145	$5.9 \cdot 10^5$	$4.1 \cdot 10^5$	$2.6 \cdot 10^5$
1,048,576	1,048,579	$2.4 \cdot 10^6$	$1.6 \cdot 10^6$	$1.1 \cdot 10^6$
Dimension $d = 4$				
scaling factor n	integration points N	$\mathbf{Y}_{\mathrm{Box}}(n)$	$\mathbf{Y}_{\mathrm{Ell}}(n)$	$\mathbf{Y}_{\mathrm{Ell}}^{*,l}(n)$
64	71	1,225	347	204
256	261	3,969	1,205	604
1,024	1,025	16,731	5,061	1,998
4,096	4,099	70,395	20,287	6,784
16,384	16,385	$2.5 \cdot 10^5$	81,105	23,756
65,536	65,533	$1.1 \cdot 10^6$	$3.2 \cdot 10^5$	86,122
262,144	262,143	$4.1 \cdot 10^6$	$1.3 \cdot 10^6$	$3.2 \cdot 10^5$
1,048,576	1,048,609	$1.7 \cdot 10^7$	$5.2 \cdot 10^6$	$1.2 \cdot 10^6$
Dimension $d = 8$				
scaling factor n	integration points N	$\mathbf{Y}_{\mathrm{Box}}(n)$	$\mathbf{Y}_{\mathrm{Ell}}(n)$	$\mathbf{Y}_{\mathrm{Ell}}^{*,l}(n)$
64	79	$2.3 \cdot 10^5$	4,459	2,359
256	271	$5.5 \cdot 10^5$	15,395	6,883
1,024	1,067	$4.1 \cdot 10^6$	63,299	18,799
4,096	4,113	$1.6 \cdot 10^7$	$2.7 \cdot 10^5$	54,411
16,384	16,413	$4.1 \cdot 10^7$	$1.1 \cdot 10^6$	$1.6 \cdot 10^5$
65,536	65,645	$2.1 \cdot 10^8$	$4.2 \cdot 10^6$	$5 \cdot 10^5$
262,144	262,263	$9.2 \cdot 10^8$	$1.7 \cdot 10^7$	$1.6 \cdot 10^6$
1,048,576	1,048,779	$3.7 \cdot 10^9$	$6.8 \cdot 10^7$	$5 \cdot 10^6$
Dimension $d = 16$				
scaling factor n	integration points N	$\mathbf{Y}_{\mathrm{Box}}(n)$	$\mathbf{Y}_{\mathrm{Ell}}(n)$	$\mathbf{Y}_{\mathrm{Ell}}^{*,l}(n)$
64	423	$9.2 \cdot 10^{10}$	$7.5 \cdot 10^5$	$7.5 \cdot 10^5$
256	967	$1.5 \cdot 10^{11}$	$4.3 \cdot 10^6$	$2.3 \cdot 10^6$
1,024	2,043	$3 \cdot 10^{11}$	$1.8 \cdot 10^7$	$7.4 \cdot 10^6$
4,096	5,835	$1.7 \cdot 10^{12}$	$5.9 \cdot 10^7$	$2.1 \cdot 10^7$
16,384	18,901	$2.4 \cdot 10^{12}$	$2.3 \cdot 10^8$	$6.5 \cdot 10^7$
65,536	69,353	$3.1 \cdot 10^{12}$	$9.7 \cdot 10^8$	$2.2 \cdot 10^8$
262,144	267,257	$6.8 \cdot 10^{12}$	$4.1 \cdot 10^9$	$6.9 \cdot 10^8$
1,048,576	1,054,837	$1.4 \cdot 10^{13}$	$1.7 \cdot 10^{10}$	$2.1 \cdot 10^9$

Figure 6: Cardinalities of the sets of Frolov-cubature points N, the bounding box $\mathbf{Y}_{\mathrm{Box}}(n)$ and the bounding ellipsoid $\mathbf{Y}_{\mathrm{Ell}}(n)$, using the Chebyshev-Frolov lattice.
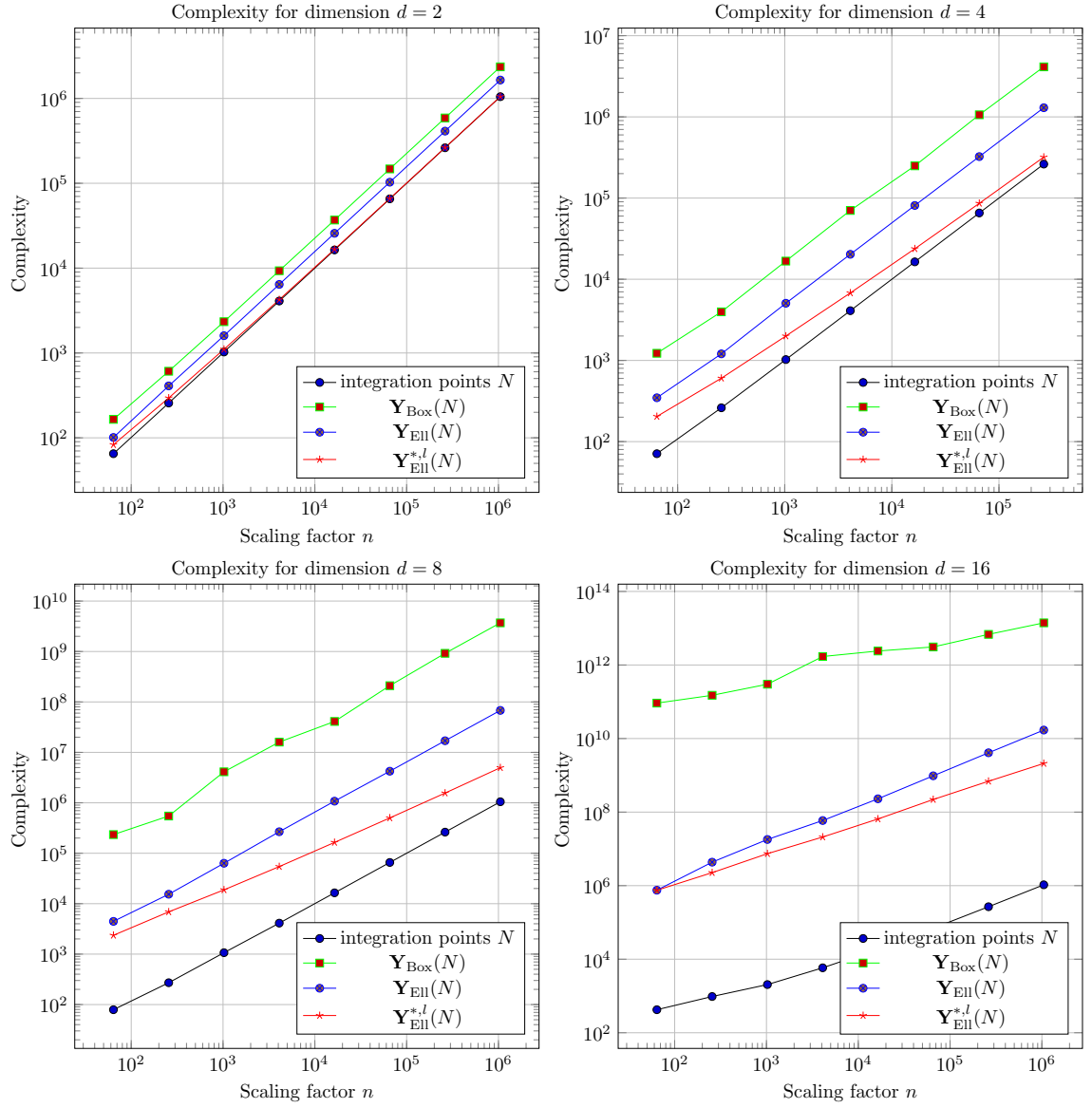
Figure 7: Complexities for dimensions $d \in \{2, 4, 8, 16\}$

6 Besov spaces of dominating mixed smoothness

In this section, we introduce the Besov spaces of dominating mixed smoothness and state the convergence properties of the Frolov cubature formula (1.9) for these function classes.

To this end, we will use a tensorized decomposition of unity $(\varphi_m)_{m \in \mathbb{N}_0^d}$ in the sense of [24, Section 1].

Definition 6.1. *Let $(\varphi_k)_{k \in \mathbb{N}} \subset \mathcal{S}(\mathbb{R})$ be a system satisfying*

$$\begin{cases} \operatorname{supp} \varphi_0 \subset \{y \in \mathbb{R} : |t| \le 2\}, \\ \operatorname{supp} \varphi_j \subset \{t \in \mathbb{R} : 2^{j-1} \le |t| \le 2^{j+1}\} & j \in \mathbb{N}, \end{cases} \tag{6.1}$$

such that for every $l \in \mathbb{N}_0$ there exists a constant c_l with

$$\|2^{jl} D^l \varphi_j(t)\|_\infty \le c_l, \quad j \in \mathbb{N}_0, \tag{6.2}$$

and

$$\sum_{j \in \mathbb{N}_0} \varphi_j \equiv 1. \tag{6.3}$$

The tensorized decomposition of unity $(\varphi_m)_{m \in \mathbb{N}_0^d}$ is then given by

$$\varphi_m(\xi) = \prod_{i=1}^d \varphi_{m_i}(\xi_i), \quad \xi \in \mathbb{R}^d. \tag{6.4}$$

Definition 6.2 (Besov space of dominating mixed smoothness)**.** *Let $1 \le p, \theta \le \infty$, $r > 0$, and $(\varphi_m)_{m \in \mathbb{N}_0^d}$ be a tensorized decomposition of unity. The Besov space of dominating mixed smoothness $S_{p,\theta}^r B = S_{p,\theta}^r B(\mathbb{R}^d)$ is the set of all $f \in L_1(\mathbb{R}^d)$ such that*

$$\|f\|_{S_{p,\theta}^r B} := \Big(\sum_{m \in \mathbb{N}_0^d} 2^{r|m|_1 \theta} \|\mathcal{F}^{-1}[\varphi_m \mathcal{F} f]\|_p^\theta \Big)^{1/\theta} < \infty \tag{6.5}$$

with the usual modification for $\theta = \infty$.

With the introduced norm, $S_{p,\theta}^r B$ is a Banach space, which embeds into the space of continuous functions for $1/p < r$. Different choices of $(\varphi_m)_{m \in \mathbb{N}_0^d}$ lead to equivalent norms; for more details we refer to [24, Theorem 1.23] and [23, Definition 2.5]. In the special case $p = \theta = 2$ we put $H_{\mathrm{mix}}^r(\mathbb{R}^d) := S_{2,2}^r B$ which denote the *Sobolev spaces of dominating mixed smoothness* r. It is well-known that for $r \in \mathbb{N}_0$, H_{mix}^r can equivalently be defined via

$$H_{\mathrm{mix}}^r(\mathbb{R}^d) = \{f \in L_2(\mathbb{R}^d) : D^\alpha f \in L_2(\mathbb{R}^d), \alpha \in \mathbb{N}_0^d, |\alpha|_\infty \le r\}, \tag{6.6}$$

which gives an idea of the properties Besov spaces exhibit. For an integration domain $\Omega \subset \mathbb{R}^d$ and $1/p < r$, we further define

$$S_{p,\theta}^r B(\Omega) = \{f \in S_{p,\theta}^r B : \operatorname{supp}(f) \subset \Omega\} \tag{6.7}$$

to be the Besov space restricted to Ω, with homogeneous boundary conditions. For $p, \theta < \infty$ it can also be regarded as the closure of $C_c^\infty(\Omega)$ with respect to the Besov norm $\|\cdot\|_{S_{p,\theta}^r B}$, cf. [17, Section 2.2.4].

The following convergence result can be found in [4, 5, 23]. Also, note the behavior of admissible lattices regarding axis-parallel boxes shown in [18].

Theorem 6.3. *Let $\Omega = [-1/2, 1/2]^d$ be the integration domain, $1/p < r$ and $\boldsymbol{B} = \{f \in S_{p,\theta}^r B(\Omega) : \|f\|_{S_{p,\theta}^r B} \le 1\}$ be the function class under consideration. Furthermore, let Γ be an admissible lattice and $\Gamma_n = (\det(\Gamma)n)^{-1/d}\Gamma$ be scaled versions thereof. Then the asymptotic relations*

$$E(\Phi_{\Gamma_n}, \boldsymbol{B}) \asymp n^{-r} \log^{(d-1)(1-1/\theta)}(n) \tag{6.8}$$

and

$$E(\Phi_{\Gamma_n}, \boldsymbol{B}) \asymp N^{-r} \log^{(d-1)(1-1/\theta)}(N) \tag{6.9}$$

hold, where $N = |\Gamma_n \cap \Omega| = n + \mathcal{O}(\log^{d-1} n)$ is the number of integration points.

The Frolov cubature formula achieves the lower bounds (1.5) and (1.6), hence it has the optimal convergence rate for Besov spaces of dominating mixed smoothness. A striking advantage is the universality of this method: it does not depend on the function space. Therefore, for a given function f, it will always realize the best convergence rate possible, i.e. it "sees" the regularity of the function f. This property actually extends to many other function classes, for instance a wide range of Triebel-Lizorkin spaces [23], which makes the Frolov cubature formula (1.9) a powerful black box method (e.g. the regularity of f may be unknown). It is also important to note that the Frolov cubature formula (1.9) can be customized to achieve the same optimal convergence rate for periodic Besov functions defined on the torus and Besov functions defined on the whole space $\mathbb{R}^d$, cf. [5].

In the following we will be concerned with the preasymptotic behavior of the Frolov cubature formula; if the constant hidden in (6.9) is too large, it may render the integration method useless. We start our analysis with Corollary 3.4, which leaves us with an explicit construction of admissible lattices for arbitrary dimension d, provided we can find a suitable polynomial $p(x) \in \mathbb{Z}[x]$. Let $\mathbf{B}$ be as in Theorem 6.3, and assume the lattice Γ to be constructed as in Corollary 3.4, with the corresponding polynomial $p(x)$ and its roots $\xi_1, \ldots, \xi_d$. For a function $f \in \mathbf{B}$, the generalized Poisson summation formula (see for instance [23, Section 3]) yields

$$\Phi_\Gamma(f) = \det(\Gamma) \sum_{x \in \Gamma \cap \Omega} f(x) = \det(\Gamma) \sum_{x \in \Gamma} f(x) = \sum_{y \in \Gamma^\perp} \mathcal{F}f(y). \tag{6.10}$$

30

Using the observation

$$\int_\Omega f(x)dx = \int_{\mathbb{R}^d} f(x)dx = \mathcal{F}f(0)\,, \tag{6.11}$$

we see that the integration error is given by

$$e(\Phi_\Gamma, f) = \Big| \sum_{y \in \Gamma^\perp \setminus \{0\}} \mathcal{F}f(y)\Big|\,. \tag{6.12}$$

The Frolov cubature formula seems to be tailored for the class **B**: On one hand, the integration error $e(\Phi_\Gamma, f)$ consists of function evaluations of the Fourier transform of f at dual lattice points $y \in \Gamma^\perp \setminus \{0\}$, which satisfy the admissibility property (2.5). On the other hand, the Besov norm $\|\cdot\|_{S^r_{p,\theta}B}$ penalizes high frequencies $\mathcal{F}f$ w.r.t. the hyperbolic cross. This core idea leads to the optimal convergence rates stated in Theorem 6.3, and also for many other function classes with similar behavior.

It is evident that the integration error decreases the higher $\mathrm{Nm}(\Gamma^\perp)$ is. We now investigate the effect the scaling of Γ has on $\mathrm{Nm}(\Gamma^\perp)$. As in Theorem 6.3, define $\Gamma_n = (\det(\Gamma)n)^{-1/d}\,\Gamma$ and consider

$$\mathrm{Nm}(\Gamma_n^\perp) = \mathrm{Nm}((\det(\Gamma)n)^{1/d}\,\Gamma^\perp) = \det(\Gamma)n\,\mathrm{Nm}(\Gamma^\perp)\,. \tag{6.13}$$

Using (3.5) we arrive at

$$\mathrm{Nm}(\Gamma_n^\perp) = \frac{n}{\det(\Gamma)}\,. \tag{6.14}$$

Theorem 3.5 implies that it is (a priori) equivalent whether one uses Φ_{Γ_n} or $\Phi_{\Gamma_n^\perp}$ as cubature formulas. Moreover, we observe that the construction given by Corollary 3.4 works better if $\det(\Gamma)$ is small. It is given by (3.4)

$$\det(\Gamma) = \prod_{k<l} |\xi_k - \xi_l|\,,$$

and we obtain another criterion for $p(x)$ to produce a "decent" lattice, namely that the roots $\xi_1, \ldots, \xi_d$ of $p(x)$ are close to each other. Finding optimal polynomials in this sense is another difficult problem; the Chebyshev-Frolov lattice is a good choice in that regard since the corresponding roots lie in $(-2, 2)$. It has determinant $d^{d/2}2^{(d-1)/2}$ (see Lemma 4.4), which is exponential in d, and here we see how the curse of dimensionality enters the picture. We will observe this effect in the next section which discusses the numerical simulations done with the Frolov cubature formula.

7 Numerical experiments

In the previous sections we have seen that the Chebyshev-Frolov lattice is admissible for dimensions $d = 2, 4, 8, 16, \ldots$ and can be used for the Frolov cubature formula (1.9). Furthermore, its orthogonality can be exploited to assemble the integration points in $\Omega = [-1/2, 1/2]^d$ up to dimension 16, applying the bounding ellipsoid approach discussed in Section 5. In this section, we will put this method to practice, using test functions belonging to different Besov spaces. A comparison with the sparse grids method will give us the opportunity to highlight the pros and cons of the Frolov cubature formula (1.9).

Sparse grids. We briefly discuss the sparse grids method for numerical integration used in our numerical experiments. For the following explanation and a general approach to sparse grids and its applications we refer to [1].
The sparse grids method can be stated recursively as

$$Q_n^{(d)} f = \sum_{i=0}^{n} \left(Q_i^{(1)} - Q_{i-1}^{(1)} \right) \otimes Q_{n-i}^{(d-1)} f, \tag{7.1}$$

where $Q_n^{(1)}$ is a one-dimensional rule, usually a compound formula of some simple rule $Q_{i,p,n}$ applied to p^n subintervals $\{[i/p^n, (i+1)/p^n] : i = 0, \ldots, p^n - 1\}$ of $[0, 1]$ respectively. As a convention one sets $Q_0^{(1)} f = f(\frac{1}{2})$ and $Q_{-1}^{(1)} f = 0$. We choose $p = 2$ and set

$$Q_{i,p,n} f = \begin{cases} \frac{1}{2p^n} \left(f(i/p^n) + f((i+1)/p^n) \right) & i \in \{1, \ldots, p^n - 2\}, \\ \frac{1}{2p^n} f(1/p^n) & i = 0, \\ \frac{1}{2p^n} f(1 - 1/p^n) & i = p^n - 1. \end{cases} \tag{7.2}$$

This essentially is the trapezoid rule model with homogeneous boundary modification. Figure 8 shows an example of our construction for $d = 2$. For our experiments, we shift $Q_n^{(d)}$ to the unit cube $[-1/2, 1/2]^d$.

Test functions. We introduce three test functions, constructed via tensorization. This allows us to easily control the regularity of a multivariate function G and normalize it to satisfy $I(G) = \int_\Omega G(x) \mathrm{d}x = 1$. This also implies that the integration error $e(A_N; G)$ and the relative integration error $e(A_N; G)/|I(G)|$ coincide. Consider the function

$$g_1 : \mathbb{R} \longrightarrow \mathbb{R}, \quad g_1(t) = \frac{3}{\sqrt{2}} \sqrt{\max\{0, 1 - |2t|\}}, \tag{7.3}$$

which is depicted in Figure 9. It is clear that g_1 has Sobolev regularity $H^r(\mathbb{R})$ with $r < 1$, but it can be shown that it also belongs to $S_{1,\infty}^r B(\mathbb{R})$ for all $r \leq 3/2$ [10]. This behavior is often observed when dealing with kink functions, i.e. functions which are continuous and piecewise smooth. The multivariate function

$$G_1(x) = \prod_{i=1}^{d} g_1(x_i) \tag{7.4}$$
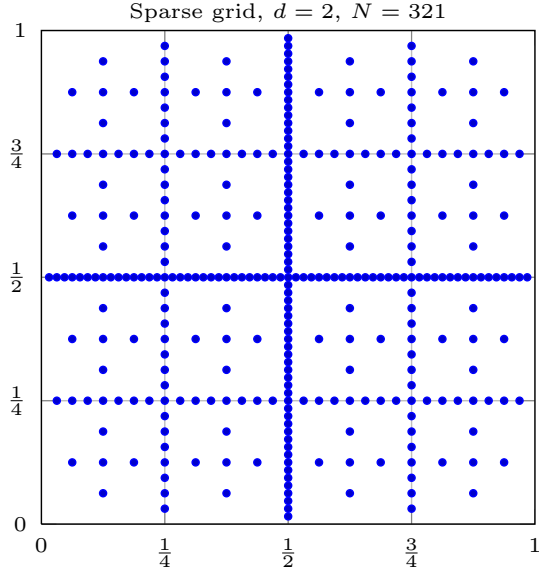
Figure 8: Trapezoid rule sparse grid for $d = 2$ with $p = 2$, $n = 5$ and number of integration points $N = 321$.

exhibits the same regularities as its univariate counterpart, i.e. $G_1 \in H^r_{\mathrm{mix}}(\mathbb{R}^d)$ with $r < 1$ and $G_1 \in S^r_{1,\infty}B(\mathbb{R}^d)$ with $r \leq 3/2$. With the convergence result (6.9) in mind, we will focus our attention on the function space $S^r_{1,\infty}B(\mathbb{R}^d)$. We expect the integration error to show the behavior

$$e(\Phi_{\Gamma_n}, G_1) \lesssim N^{-3/2} \log^{d-1}(N). \tag{7.5}$$

In Figure 12 we computed the relative error of the Frolov cubature formula (1.9) and the sparse grids method using G_1 as input for the dimensions $d \in \{2, 4, 8, 16\}$. For all dimensions, we see that the Frolov cubature formula achieves the predicted convergence rate. Concerning preasymptotic, the sparse grids method has the upper hand, but in the long run the Frolov cubature formula clearly outclasses the sparse grids method. This can be explained by the extra logarithmic term appearing in the convergence rate of the sparse grids method (1.8), which is depending on the smoothness r. The main rate N^{-r} is strongly influenced by this logarithmic term because the smoothness $r = 3/2$ is small for $G_1(x)$. For increasing dimension d, both methods need an increasing amount of integration points N to achieve a decent integration error. In dimension $d = 16$, the displayed sparse grids behavior is clearly governed by preasymptotics, whereas the Frolov cubature formula only achieves an integration error of 10^{-2}. We can see that the curse of dimensionality significantly affects the constant involved in the convergence rate (6.9). In Section 6 we saw that the constant is affected by the initial determinant of the Chebyshev-Frolov lattice, which depends exponentially on d. Another reason may be our choice of normalization. We chose our test function to satisfy $I(G_1) = 1$, but the Besov-norm $\|G_1\|_{S^r_{1,\infty}B}$ may be large because it is depending exponentially

33
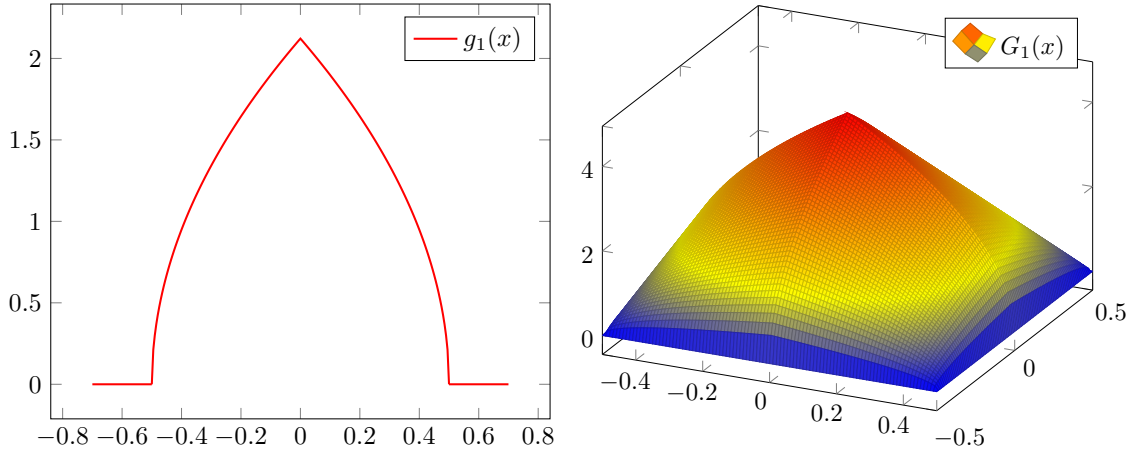
Figure 9: The univariate function $g_1(x)$ (left) and the tensorized function $G_1(x)$ for $d = 2$ (right).

on d due to our tensorization technique. On the other hand, normalizing with respect to a specific Besov-norm (6.5) is difficult because it is not easy to evaluate such an expression. We continue with the univariate function

$$g_2(t) = \frac{15\sqrt{5}}{4} \max\left\{\frac{1}{5} - t^2, 0\right\}, \tag{7.6}$$

which belongs to $S_{1,\infty}^r B(\mathbb{R})$ with $r = 2$ and has normalized integral. The tensorized function

$$G_2(x) = \prod_{i=1}^{d} g_2(x_i) \tag{7.7}$$

again has Besov regularity $r = 2$ and was also discussed in [10], see also Figure 10. In Figure 13 we computed the relative error of the Frolov cubature formula (1.9) and the sparse grids method using G_2 as input for the dimensions $d \in \{2, 4, 8, 16\}$. For dimensions $d = 2, 4, 8$, we see that the Frolov cubature formula achieves the predicted convergence rate. For $d = 16$ this is not the case, this time both the Frolov cubature formula and the sparse grids method show preasymptotic behavior. For $d = 2, 4, 8$, after a preasymptotic phase the Frolov cubature formula performs better than the sparse grid method, but the margin seems to be smaller if we compare this to Figure 12 and $G_1(x)$. This may be due to the higher smoothness parameter $r = 2$, resulting in a stronger main rate and a smaller influence of the logarithmic extra term. We will try to verify this with our next test function

$$g_3(z) = 3\mathcal{X}_{[-1/2,1/2]} * \mathcal{X}_{[-1/2,1/2]} * \mathcal{X}_{[-1/2,1/2]}(3z), \tag{7.8}$$

where $\mathcal{X}_{[-1/2,1/2]}$ is the characteristic function w.r.t. $[-1/2, 1/2] \subset \mathbb{R}$. This threefold convo-

34
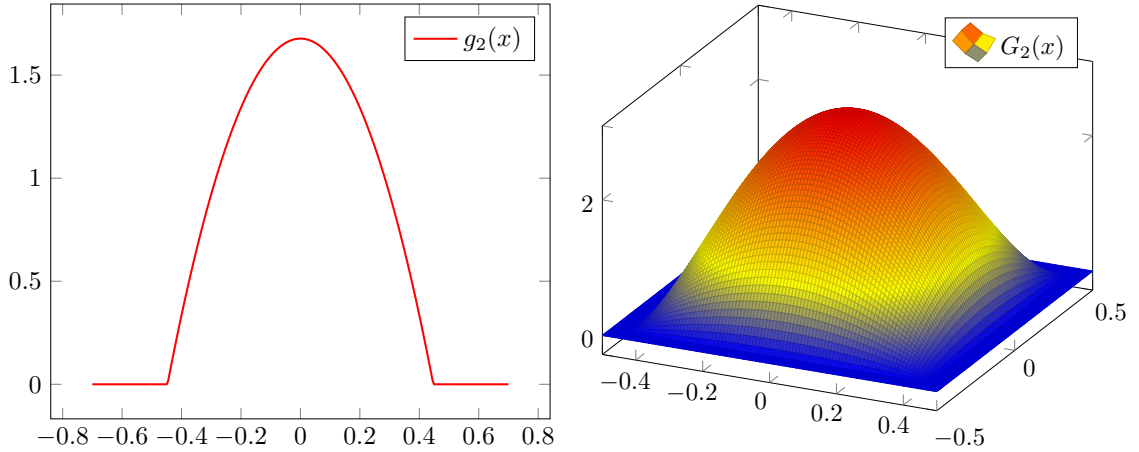
Figure 10: The univariate function $g_2(x)$ (left) and the tensorized function $G_2(x)$ for $d = 2$ (right).

lution belongs to $S_{1,\infty}^r B(\mathbb{R})$ with $r = 3$. Therefore the tensorized version

$$G_3(x) = \prod_{i=1}^{d} g_3(x_i) \tag{7.9}$$

is an element of $S_{1,\infty}^r B(\mathbb{R}^d)$ (see also Figure 11). In Figure 14 we computed the relative error of the Frolov cubature formula (1.9) and the sparse grids method using G_3 as input for the dimensions $d \in \{2, 4, 8, 16\}$. As above, one can see that the Frolov cubature formula achieves the predicted convergence rate. For $d = 16$ both the Frolov cubature formula and the sparse grids method show preasymptotic behavior. For $d = 2, 4, 8$, after a preasymptotic phase the Frolov cubature formula performs better than the sparse grid method, however, we see that this preasymptotic phase is long for dimension $d = 8$. Overall, these convergence plots seem to be more similar to those of $G_2(x)$, which would indicate that the logarithmic term in the case $r = 3/2$ is the reason for the larger difference in convergence rates.

For all functions, we observe that the behavior in dimension $d = 16$ is similar and independent of the regularity. To investigate this further, we briefly introduce another 3 functions defined on $[-1/2, 1/2]^d$ via

$$G_4(x) = \prod_{i=1}^{d} \frac{2}{\pi} \sin\left(\pi\left(x_j + \frac{1}{2}\right)\right)$$

$$G_5(x) = \prod_{i=1}^{d} 0.763 \sin\left(\pi\left(x_j + \frac{1}{2}\right)\right)^{\frac{1}{2}}$$

$$G_6(x) = \prod_{i=1}^{d} 0.222 \exp\left(\frac{1}{1 - (2(x_j + \frac{1}{2}) - 1)^2}\right)$$

35
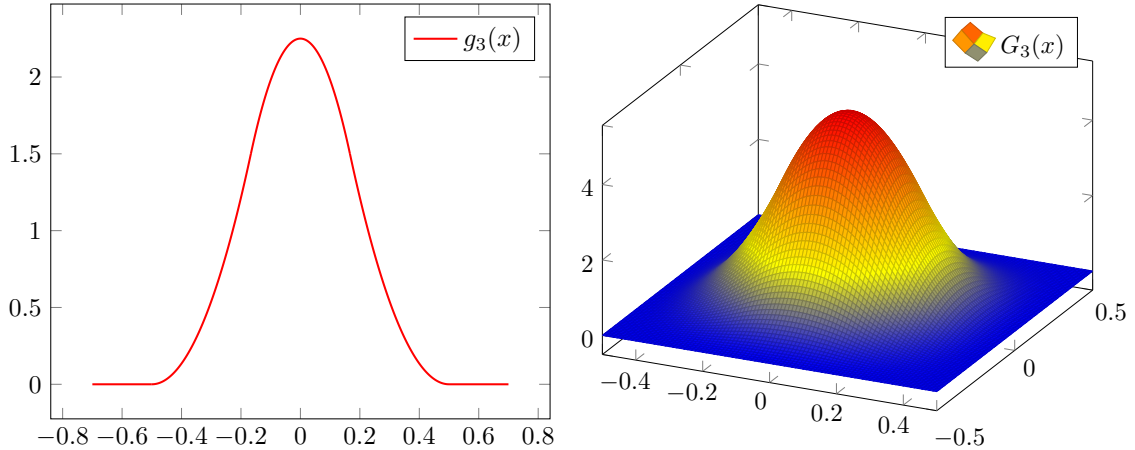
Figure 11: The univariate function $g_3(x)$ (left) and the tensorized function $G_3(x)$ for $d = 2$ (right).

and extended by 0 to $\mathbb{R}^d$. The constants were computed up to machine precision to satisfy $\int_\Omega G(x)\mathrm{d}x = 1$ and appear rounded in the above definitions. $G_4(x)$ is smooth up to kinks at the boundary of Ω and therefore behaves like $G_2(x)$, the difference lying in the placement of the kink. $G_5(x)$ has the same structure as $G_1(x)$, but without the kink at 0. $G_6(x)$ belongs to $C_c^\infty(\mathbb{R}^d)$ and therefore is an element of $S_{1,\infty}^r B(\mathbb{R}^d)$ for any smoothness parameter r. In this case we expect the convergence rate to be better than polynomial, however there are no theoretical results backing this up so far. In Figure 15 we see the relative integration error of the Frolov cubature formula for the introduced functions, for dimensions $d \in \{2, 4, 8, 16\}$. While for low dimensions the convergence behavior is well distinguished and ordered by smoothness, it is getting harder to differentiate it for higher dimensions. At dimension $d = 16$, all functions have essentially the same convergence plot, only with a varying constant. This indicates that in dimension $d = 16$, our integration point set is way too small, resulting in a display of preasymptotic behavior for all considered functions. The constant does not seem to depend on the regularity of the function, but rather on the distribution of "mass" of a given function. The functions with a small constant G_1 and G_5 have relatively high function values up to the boundary of Ω, and moderately high values around 0. On the other hand, the function with the highest constant G_3 has very small values around the boundary of Ω, and it is the function which suffers the most from the pinpoint-effect induced by our tensorization construction. This overall behavior has its reason most likely in the fact that at dimension $d = 16$, for small integration point sets almost all points except 0 lie close to the boundary of Ω, whereas the "mass" of the function is concentrated around 0 for our functions. It would be interesting to know if one can get a good estimate on the preasymptotic behavior of the Frolov cubature formula, relying only on the mass distribution of a function.

36
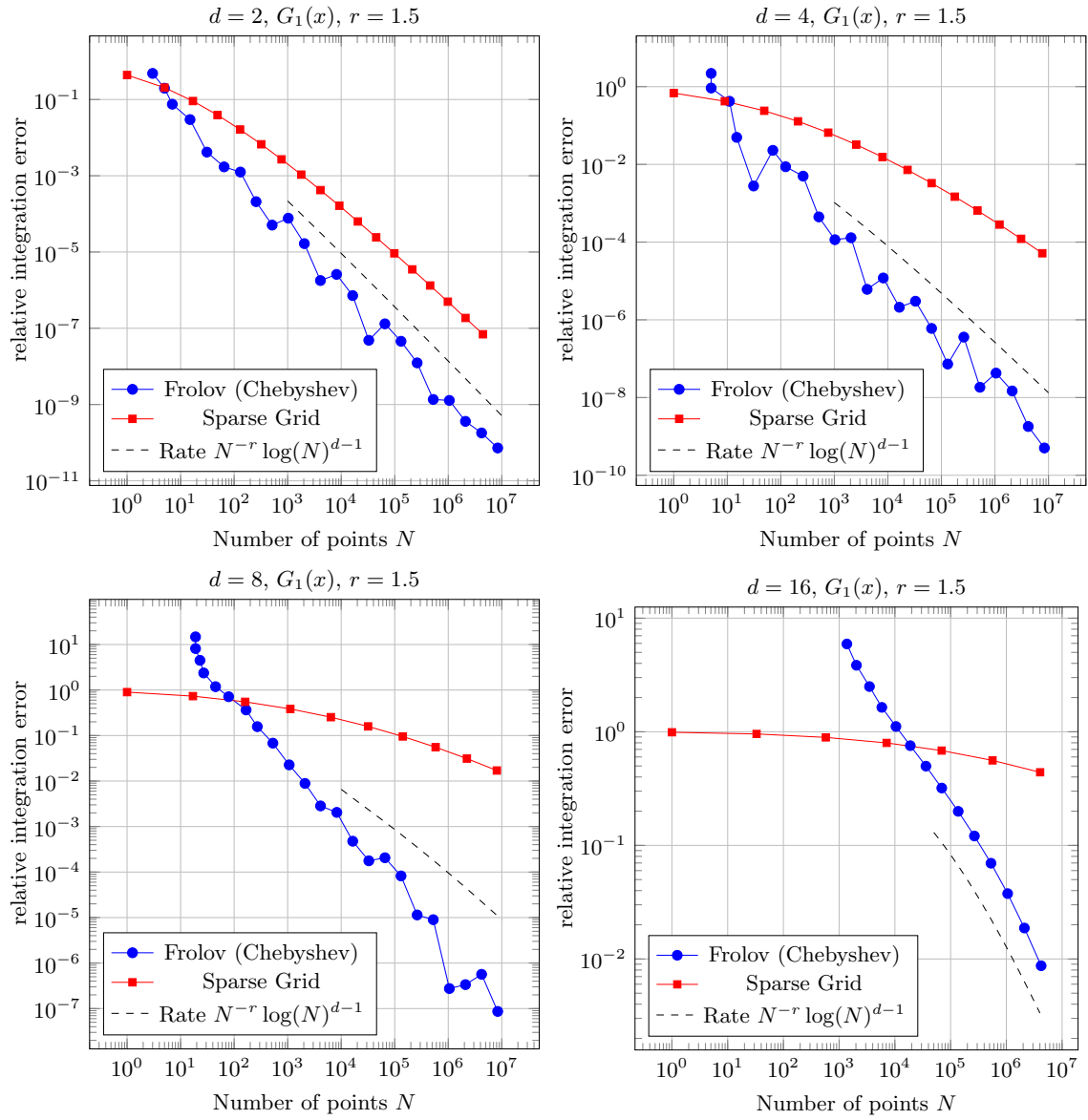
Figure 12: relative integration error for the function $G_1(x)$
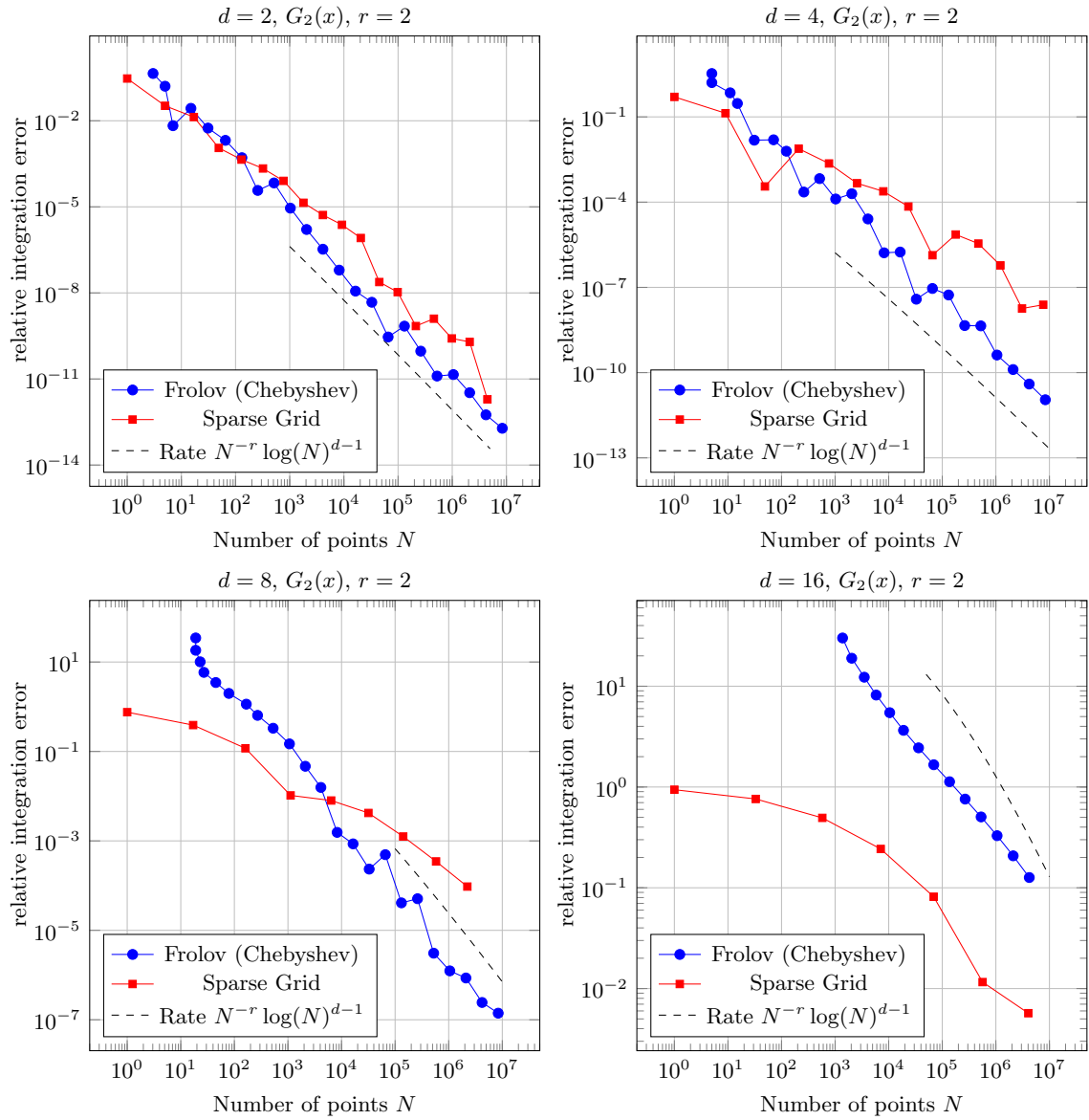
Figure 13: relative integration error for the function $G_2(x)$
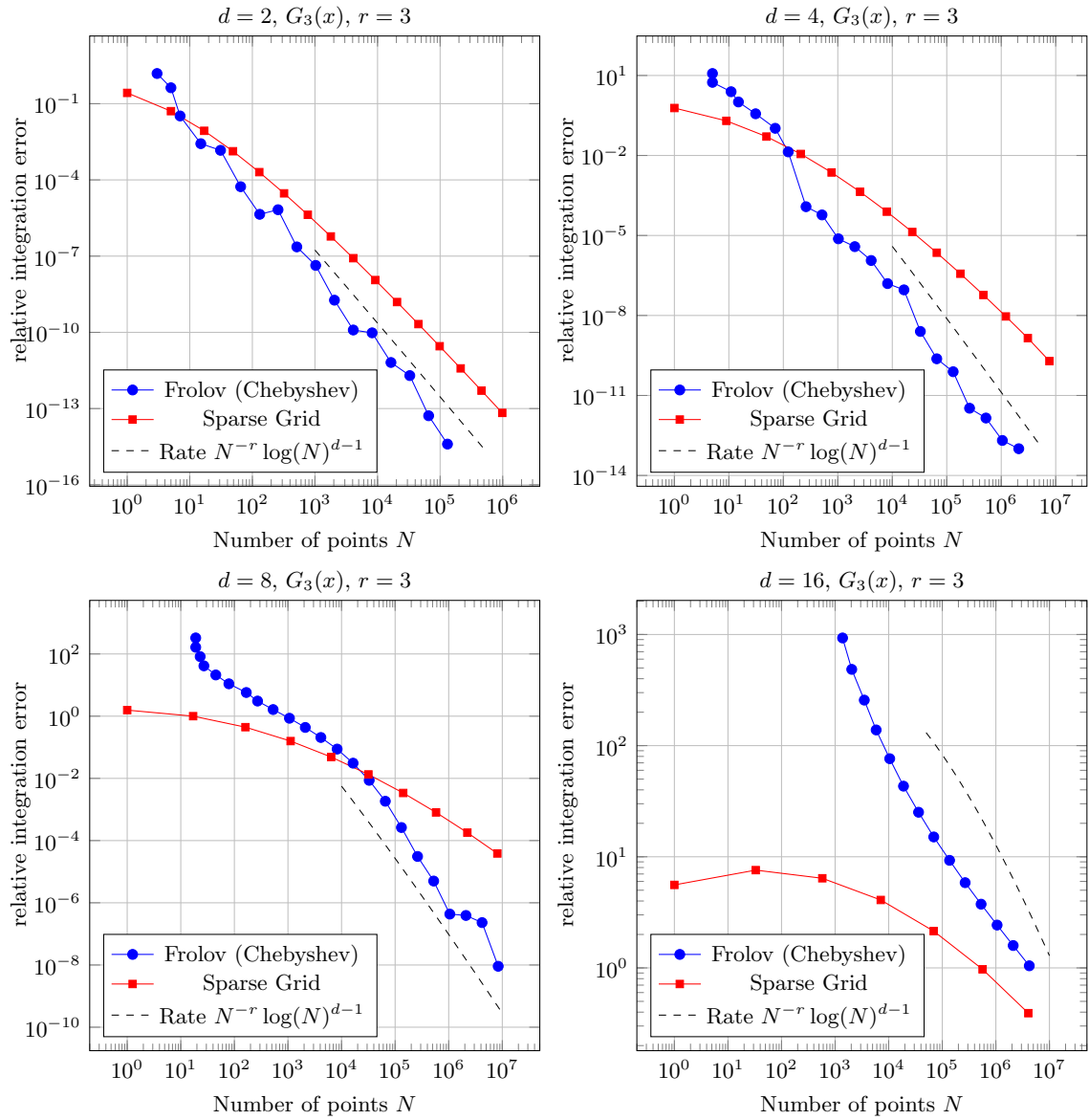
Figure 14: relative integration error for the function $G_3(x)$
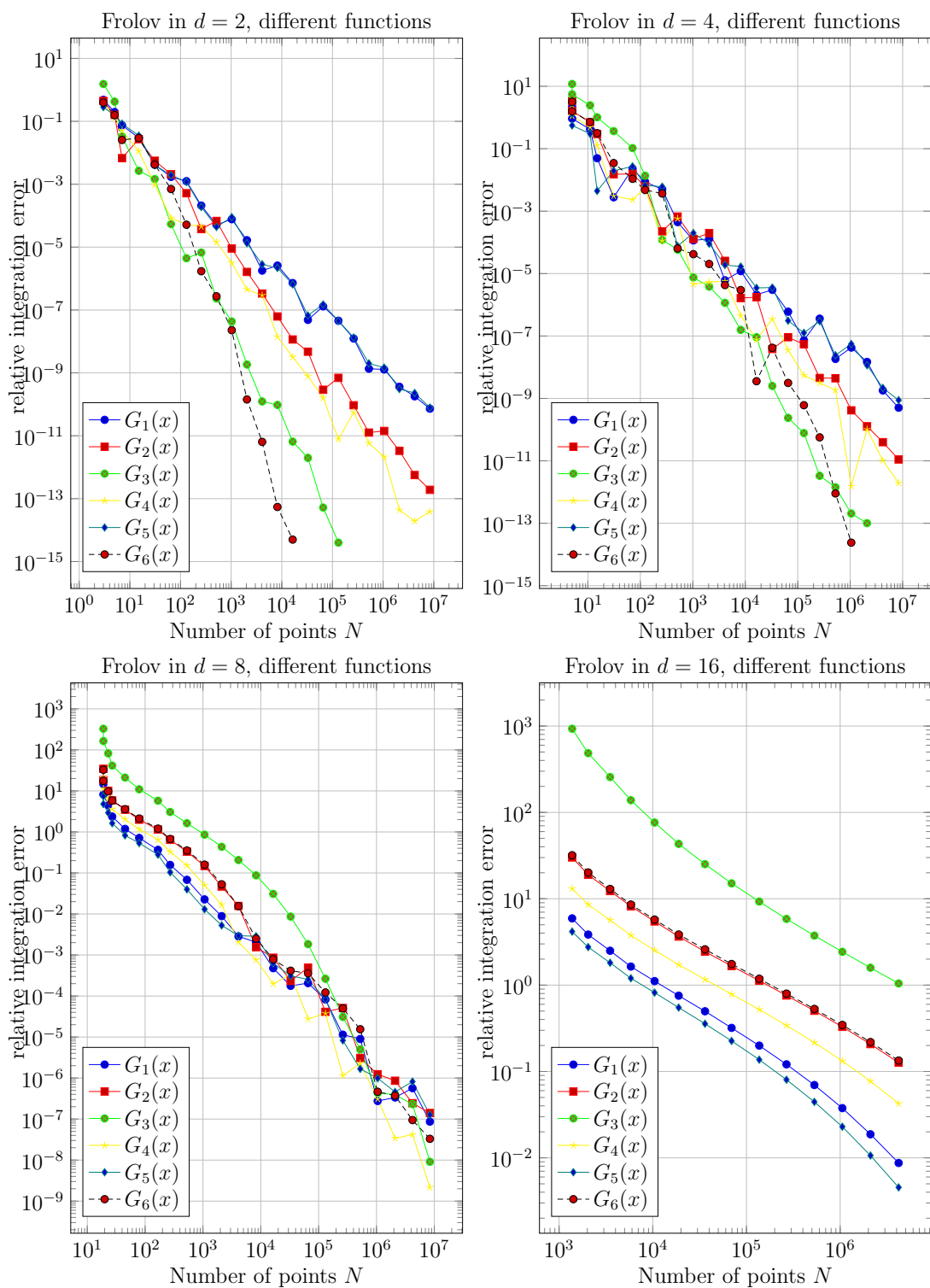
Figure 15: relative integration error for all considered functions using the Frolov cubature formula

8 Conclusion

Summary. From the theoretical point of view, the Frolov cubature formula (1.9) is an attractive high dimensional integration scheme, because it achieves optimal convergence rates for a wide range of function classes, especially those of dominating mixed smoothness type. The realization of this method however is no easy task, as we demonstrated over the course of this thesis.

A certain degree of lattice and number theory is necessary to construct lattices with the admissibility property. Corollary 3.4 provides us with a construction method of Vandermonde-type lattices which are admissible, but it is only partially explicit, in the sense that we need to find specific polynomials from which the admissible lattice is constructed. For dimensions $d = 2^m, m \in \mathbb{N}$, scaled Chebyshev polynomials fit the criteria of Corollary 3.4, and the resulting Chebyshev-Frolov lattice can be used for the Frolov cubature formula. Moreover, the roots of the scaled Chebyshev polynomials fall into the interval $(-2, 2)$, which not only induces a small determinant of the lattice, but also allows us to easily compute a good lattice representation matrix with small entries in a numerically stable way. The most surprising fact though is that this matrix has orthogonal column vectors, i.e. the Chebyshev-Frolov lattice is orthogonal.

If the lattice and a suitable representation is chosen, the next step is to assemble the integration points for the Frolov cubature formula. This necessary preprocessing step is not an easy task and may result in a long computation time. Using the orthogonality property of the Chebyshev-Frolov lattice, we revised an algorithm to enumerate the integration points in an efficient manner, called the bounding ellipsoid approach. We are now able to use the Frolov cubature formula in dimensions $2, 4, 8$ and 16.

The numerical experiments have shown that the Frolov cubature formula demonstrates its good points in long time behavior, because it achieves optimal convergence rates for Besov-type functions of arbitrary high smoothness, and in its universality, i.e. detecting the correct smoothness of a given function. One obvious bad point though is its preasymptotic behavior. High initial constants and long preasymptotic periods of the integration error make it questionable whether the Frolov cubature formula is viable for high dimensions. The generalizations mentioned in [5, 16] will only worsen this effect. For moderately high dimensions $d \leq 10$ the Frolov cubature formula can certainly be practicable, provided one can find good polynomials to make use of Corollary 3.4 and efficiently assemble the integration points.

Outlook. The most important future plan regarding the Frolov cubature formula would be a prolonged experimental phase. The numerical experiments presented in this thesis are by no means exhaustive, and the successful implementation allows us to investigate convergence behavior on function classes which were not considered in this thesis, or even in the

theory revolving around the Frolov cubature formula. Especially the function class of smooth functions with compact support seems to be interesting. In a more general view, the limitation to functions with compact support is rather restricting. The implementation of the Frolov cubature formula for periodic Besov spaces and Besov spaces with arbitrary boundary conditions mentioned in [5, 16] would greatly increase the practicability of this method. It would also allow for a more thorough investigation of convergence behavior.

Another interesting modification of the Frolov cubature formula is given by randomization [12, 22]. The lattice in use is dilated and shifted randomly, placing this variant closer to the Monte-Carlo integration schemes. However, putting this method to practice is only possible if efficient assemblation strategies for general affine lattices are available, because every realization of the random lattice produces a different set of integration points. In this case, we cannot rely on the orthogonality of e.g. the Chebyshev-Frolov lattice any more, because a random dilation would nullify this property. To solve this problem, one could either find a better bounding set, or somehow generalize the bounding ellipsoid approach.

Finally, for dimensions which are not a power of 2 one needs to find suitable polynomials which can be used to construct admissible lattices via Corollary 3.4, preferably with roots that lie close to each other. For dimensions d which satisfy that $2d + 1$ or $d + 1$ is a prime number, there are decent polynomials available, and this will hopefully make the dimensions $d \in \{3, 5, 6, 9, 10, 11, 12, 14, 15\}$ available for our experiments. The missing dimensions $7, 13 \ldots$ seem to be in need of special treatment.

References

[1] H.-J. Bungartz and M. Griebel. Sparse Grids. *Acta Numerica*, pages 1–123, 2004.

[2] J. Dick and F. Pillichshammer. *Digital Nets and Sequences: Discrepancy Theory and Quasi-Monte Carlo Integration.* Cambridge University Press, 2010.

[3] V. Dubinin. Cubature formulas for classes of functions with bounded mixed difference. *Math. USSR Sbornik 76*, pages 283–292, 1993.

[4] V. Dubinin. Cubature formulae for Besov classes. *Izvestiya Math 61(2)*, pages 259–283, 1997.

[5] D. Dũng, V. Temlyakov, and T. Ullrich. Hyperbolic cross approximation. *ArXiv e-prints*, Jan. 2016.

[6] D. Dũng and T. Ullrich. Lower bounds for the integration error for multivariate functions with mixed smoothness and optimal Fibonacci cubature for functions on the square, 2013.

[7] K. K. Frolov. Upper bounds for the errors of quadrature formulae on classes of functions. *Dokl. Akad. Nauk SSSR*, 231(4):818–821, 1976.

[8] T. Goda, K. Suzuki, and T. Yoshiki. Optimal order quadrature error bounds for infinite-dimensional higher order digital sequences, 2016.

[9] P. M. Gruber and C. G. Lekkerkerker. *Geometry of numbers*, volume 37 of *North-Holland Mathematical Library*. North-Holland Publishing Co., Amsterdam, second edition, 1987.

[10] A. Hinrichs, L. Markhasin, J. Oettershagen, and T. Ullrich. Optimal quasi-Monte Carlo rules on order 2 digital nets for the numerical integration of multivariate periodic functions. 2015.

[11] C. Kacwin, J. Oettershagen, and T. Ullrich. On the orthogonality of the Chebyshev-Frolov lattice and applications, 2016.

[12] D. Krieg and E. Novak. A universal algorithm for multivariate integration. *Foundations of Computational Mathematics*, to appear.

[13] A. K. Lenstra, H. W. Lenstra, and L. Lovász. Factoring polynomials with rational coefficients. *Mathematische Annalen*, 261(4):515–534, 1982.

[14] U. Luther and K. Rost. Matrix exponentials and inversion of confluent Vandermonde matrices. *Electron. Trans. Num. Anal 18*, pages 91–100, 2004.

[15] D. A. Marcus. *Number Fields (Universitext).* Springer, 1995.

[16] V. Nguyen, M. Ullrich, and T. Ullrich. Change of variable in spaces of mixed smoothnes and numerical integration of multivariate functions on the unit cube. *Arxive preprints*, 2015.

[17] H.-J. Schmeisser and H. Triebel. *Topics in Fourier Analysis and Function Spaces*. John Wiley and Sons, 1987.

[18] M. M. Skriganov. Constructions of uniform distributions in terms of geometry of numbers. *Algebra i Analiz*, 6(3):200–230, 1994.

[19] S. A. Smolyak. Quadrature and interpolation formulas for tensor products of certain classes of functions. *Dokl. Akad. Nauk SSSR*, 4:240–243, 1963.

[20] V. Temlyakov. Approximation of functions with bounded mixed derivative. *Proc. Steklov Inst. Math.*, (1(178)):vi+121, 1989. A translation of Trudy Mat. Inst. Steklov **178** (1986), Translated by H. H. McFaden.

[21] V. N. Temlyakov. *Approximation of periodic functions*. Computational Mathematics and Analysis Series. Nova Science Publishers, Inc., Commack, NY, 1993.

[22] M. Ullrich. A monte carlo method for integration of multivariate smooth functions i: Sobolev spaces, 2016.

[23] M. Ullrich and T. Ullrich. The role of Frolov's cubature formula for functions with bounded mixed derivative. *SIAM Journ. on Numerical Analysis*, to appear.

[24] J. Vybíral. Function spaces with dominating mixed smoothness. *Dissertationes Math.*, 436:73 pp., 2006.